

A new dipolar potential for numerical simulations of polar fluids on the 4D hypersphere.

Jean-Michel Caillol*

Univ. Paris-Sud, CNRS, LPT, UMR 8627, Orsay, F-91405, France

Martin Trulsson†

Univ. Paris-Sud, CNRS, LPTMS, UMR 8626, Orsay, F-91405, France

(Dated: August 16, 2021)

Abstract

We present a new method for Monte Carlo or Molecular Dynamics numerical simulations of three dimensional polar fluids. The simulation cell is defined to be the surface of the northern hemisphere of a four-dimensional (hyper)sphere. The point dipoles are constrained to remain tangent to the sphere and their interactions are derived from the basic laws of electrostatics in this geometry. The dipole-dipole potential has two singularities which correspond to the following boundary conditions : when a dipole leaves the northern hemisphere at some point of the equator, it reappears at the antipodal point bearing the same dipole moment. We derive all the formal expressions needed to obtain the thermodynamic and structural properties of a polar liquid at thermal equilibrium in actual numerical simulation. We notably establish the expression of the static dielectric constant of the fluid as well as the behavior of the pair correlation at large distances. We report and discuss the results of extensive numerical Monte Carlo simulations for two reference states of a fluid of dipolar hard spheres and compare these results with previous methods with a special emphasis on finite size effects.

Keywords: Hypersphere; Monte Carlo simulations; Polar fluids; Dielectric constant

*Electronic address: Jean-Michel.Caillol@th.u-psud.fr

†Electronic address: Martin.Trulsson@u-psud.fr

I. INTRODUCTION

Numerical simulation of Coulomb fluids -by this terminology we mean fluids made of charged or (and) polar molecules- need special precaution because of the long range of electrostatics interactions. Various technical solutions to this problem have been proposed. The most common one is to consider a cubic simulation cell with periodic boundary conditions in conjunction with Ewald summation techniques [1, 2]. An alternative consists in confining particles at the surface \mathcal{S}_3 of a four-dimensional (4D) sphere - a hypersphere for short [2–6]. The 3D non-Euclidian space \mathcal{S}_3 , albeit finite, is homogeneous and isotropic, in the sense that it is invariant under the group $\mathcal{O}(4)$ of the 4D rotations; it is thus well suited for the simulation of liquids. Moreover, electrostatics can easily be developed in \mathcal{S}_3 and, in particular, the Green function of Laplace equation can be computed analytically and it has a very simple expression, tailor-made for numerical evaluations.

The present paper is devoted to dipolar fluids and we propose a new dipole-dipole potential in \mathcal{S}_3 with some advantages over the versions considered in previous studies [3–6].

A brief reminder on the electrostatics in \mathcal{S}_3 should be useful for a better understanding of these issues. We know from Landau [7] that, in a finite space such as \mathcal{S}_3 , the total electric charge must be equal to zero. Therefore, the building brick of electrostatics cannot be a single point charge as we are used to in the ordinary Euclidian space \mathbf{E}_3 . A first possibility is to consider rather a pseudo-charge, a neologism denoting the association of a point charge and a uniform neutralizing background of opposite charge. It turns out that the electric potential and field of a pseudo-charge can be computed analytically. Various models of statistical mechanics involving electric charges can therefore be easily simulated in \mathcal{S}_3 . For instance, the one component plasma (OCP) -*i.e.* an assembly of point charges of the same sign immersed in a uniform neutralizing continuum- may be seen as an assembly of N identical pseudo-charges, the individual neutralizing back-grounds of the pseudo-charges adding up to constitute the total neutralizing bath of the model. High precision Monte Carlo (MC) simulations of the thermodynamic and structural properties of the OCP have been obtained by MC simulations of a collection of pseudo-charges living in \mathcal{S}_3 [8]. Of course multipolar interactions are easily derived from these basic Coulomb interactions and more complex Coulomb fluids such as polar fluids or electrolytes can be and have actually been simulated before in \mathcal{S}_3 , see *e.g.* [3–6].

In an alternative construction of electrostatics, proposed in Ref. [9], the "building brick" is composed of a bi-charge, *i.e.* a dumbbell made of two antipodal charges of opposite signs $+q$ and $-q$. The potential of a bi-charge is obtained as a solution of Laplace-Beltrami equation in \mathcal{S}_3 . It has two singularities, one at the north pole, the other at the south pole. A system of dumbbells living on the whole sphere \mathcal{S}_3 is equivalent to a mixture of charges $+q$ and $-q$ leaving on the northern hemisphere \mathcal{S}_3^+ . We then have the peculiar boundary conditions : when the positive charge of the dumbbell leaves the northern hemisphere \mathcal{S}_3^+ at some point M of the equator, the negative charge of the dumbbell reappears at the antipodal point \bar{M} ($\overrightarrow{OM} = -\overrightarrow{O\bar{M}}$, O center of the sphere), Some models with special symmetries can be considered as made of bi-charges. For instance the restricted primitive model (RPM) of electrolytes, *i.e.* an equimolar mixture of anions and cations of the same valence can be represented by a simple fluid of identical bi-charges of \mathcal{S}_3 (provided admittedly that the anions and cations have the same diameter). The extensive MC simulations of the Orsay group on the critical point of the RPM have all been done in this geometry [10]. In the present work, bi-dipoles are built from bi-charges and used to perform actual MC simulations of dipolar hard spheres (DHS). A fluid of bi-dipoles living on the whole surface of a hypersphere is clearly equivalent to a fluid of ordinary mono-dipoles living on the northern hemisphere of \mathcal{S}_3 . When a dipole leaves the hemisphere at some point M of the equator it reenters the hemisphere at the antipodal point \bar{M} , bearing the same dipolar vector.

Our paper is organized as follows. In Sec. (II) we summarize the main mathematical tools needed in the remainder of the article. We are then well equipped to build the electrostatics in space \mathcal{S}_3 in Sec. (III); starting from Poisson's equation we obtain the potentials and fields of bi-charges and, by differentiation that of bi-dipoles. We then specialize our purpose in Sec. (IV) to the DHS model in \mathcal{S}_3 and derive all formal expressions needed in MC simulations. In particular we obtain a family of formula relating the dielectric constant to the polarization fluctuations. We also obtain the asymptotic behavior of the pair correlation function at thermal equilibrium. In Sec. (V) we present extensive MC simulations of a DHS fluid. The models of mono and bi-dipoles in \mathcal{S}_3 are compared with the the usual DHS fluid in cubico-periodical geometry. Finite size effects on thermodynamical properties, the dielectric constant and the pair correlation functions are studied in great detail for two reference thermodynamic states. We conclude in Sec. (VI).

II. POINTS, VECTORS, TENSORS AND FUNCTIONS ON THE HYPER-SPHERE

A. Points and Geodesics

The simplest and most fruitful point of view is to consider the hypersphere $\mathcal{S}_3(O, R)$ of center O and radius R as a trivial generalization of the sphere $\mathcal{S}_2(O, R)$ of the usual 3D geometry. Mathematically, it is a compact manifold of the 4D Euclidian space E_4 (to be identified with \mathbf{R}^4), defined as the subset of points $\mathbf{OM} = R (z_1, z_2, z_3, z_4)^T$ which satisfy to the constraint $z_1^2 + z_2^2 + z_3^2 + z_4^2 = 1$. When we have in mind the hypersphere of unit radius we adopt the uncluttered notation $\mathcal{S}_3 \equiv \mathcal{S}_3(O, R = 1)$. Elementary geometric constructs, valid for the sphere $\mathcal{S}_2(O, R)$, can easily be extended to the 4D case [3, 4, 11] and replace more sophisticated mathematical tools used to deal with general Riemannian manifolds.

In $\mathcal{S}_3(O, R)$ the distance r_{12} between two points M_1 and M_2 is defined as the length of the shortest path in the space $\mathcal{S}_3(O, R)$, *i.e.* the geodesic M_1M_2 , linking these two points; it is a bit of the unique circle of center O and radius R which passes through the two points. One easily finds that

$$r_{12}/R = \psi_{12} = \cos^{-1}(\mathbf{z}_1 \cdot \mathbf{z}_2) , \quad (1)$$

where $\mathbf{z}_i = \mathbf{OM}_i/R$, $i = 1, 2$ and $0 \leq \psi_{12} \leq \pi$. We denote by $\mathbf{t}_{12}(M_1)$ and $\mathbf{t}_{12}(M_2)$ the two unit vectors tangent to the geodesic M_1M_2 , respectively at points M_1 and M_2 . By convention, the arrows of the vectors point from M_1 towards M_2 . One has [11]

$$\mathbf{t}_{12}(M_1) = +\frac{\mathbf{z}_2}{\sin \psi_{12}} - \mathbf{z}_1 \cot \psi_{12} , \quad (2a)$$

$$\mathbf{t}_{12}(M_2) = -\frac{\mathbf{z}_1}{\sin \psi_{12}} + \mathbf{z}_2 \cot \psi_{12} . \quad (2b)$$

Note that both vectors $\mathbf{t}_{12}(M_1)$ and $\mathbf{t}_{12}(M_2)$ are undefined for $\psi_{12} = 0$ or $\psi_{12} = \pi$. In the latter case M_1 and M_2 are two antipodal points and there is an infinity of geodesics, all of length $R\pi$, connecting the two points. Henceforth we shall note \overline{M}_1 the antipodal point.

B. Spherical coordinates

The generic unit vector $\mathbf{z} = \mathbf{OM}/R$ of \mathcal{S}_3 can be conveniently written in spherical coordinates as $\mathbf{z} = (\sin w \sin v \cos u, \sin w \sin v \sin u, \sin w \cos v, \cos w)^T$ with $0 \leq w, v \leq \pi$ and

$0 \leq u < 2\pi$. The angle w determines the distance Rw of point M from the north pole N of the sphere $\mathcal{S}_3(O, R)$. *i.e.* the length of the geodesy NM [12]. The differential vector $d\mathbf{z}$ of point \mathbf{z} of \mathcal{S}_3 is easily found to be

$$d\mathbf{z} = dw \mathbf{e}_w + \sin w dv \mathbf{e}_v + \sin w \sin v du \mathbf{e}_u , \quad (3)$$

with

$$\mathbf{e}_w \equiv \partial\mathbf{z}/\partial w = (\cos w \sin v \cos u, \cos w \sin v \sin u, \cos w \cos v, -\sin w)^T , \quad (4a)$$

$$\mathbf{e}_v \equiv (\partial\mathbf{z}/\partial v)/\sin w = (\cos v \cos u, \cos v \sin u, -\sin v, 0)^T , \quad (4b)$$

$$\mathbf{e}_u \equiv (\partial\mathbf{z}/\partial u)/(\sin w \sin v) = (-\sin u, \cos u, 0, 0)^T . \quad (4c)$$

The 3 orthonormal vectors $(\mathbf{e}_u, \mathbf{e}_v, \mathbf{e}_w)$ constitute the "local basis" of \mathcal{S}_3 in spherical coordinates. This basis spans the 3D Euclidian space $\mathcal{T}_3(M)$, tangent to the hypersphere at point M . To make some contact with the material of section (II A) we note that $\mathbf{e}_w(\mathbf{z}) = \mathbf{t}_{NM}(M)$ is the unit vector, tangent at the geodesic NM at point M . Moreover one checks readily that it satisfies identity (2b).

It also follows from Eq. (3) that the infinitesimal length element of $\mathcal{S}_3(O, R)$ is $ds^2 = \sin^2 w \sin^2 u du^2 + \sin^2 w dv^2 + dw^2$ and that the infinitesimal volume element takes the simple form $d\tau = R^3 d\Omega = R^3 \sin^2 w \sin v du dv dw$, so that the total volume of space $\mathcal{S}_3(O, R)$ is $V_{\text{Tot.}} = \int d\tau = 4\pi^2 R^3$.

It is in place to define the unit dyadic tensor $\mathbf{U}_{\mathcal{S}_3}(\mathbf{z}) = \mathbf{e}_u \mathbf{e}_u + \mathbf{e}_v \mathbf{e}_v + \mathbf{e}_w \mathbf{e}_w$ of the tangent Euclidian space $\mathcal{T}_3(\mathbf{z})$; note that the unit dyadic tensor of Euclidian space \mathbf{E}_4 is clearly given by $\mathbf{U}_{\mathbf{R}^4} = \mathbf{U}_{\mathcal{S}_3}(\mathbf{z}) + \mathbf{z}\mathbf{z}$. These admittedly old-fashioned objects however allow an easy definition of the gradient in \mathcal{S}_3 , or first differential Beltrami operator, as

$$\nabla_{\mathcal{S}_3} = \mathbf{U}_{\mathcal{S}_3}(\mathbf{z}) \cdot \nabla_{\mathbf{R}^4} ,$$

where $\nabla_{\mathbf{R}^4}$ is the usual Euclidian gradient operator of \mathbf{R}^4 and the dot in the r.h.s. denotes the 4D tensorial contraction. Note that the gradient in the hypersphere $\mathcal{S}_3(O, R)$ of radius $R \neq 1$ is of course defined as $\nabla_{\mathcal{S}_3(O, R)} = \nabla_{\mathcal{S}_3}/R$.

The Laplace-Beltrami operator (or second differential Beltrami operator) will be similarly defined as the restriction of the 4D Laplacian $\Delta_{\mathbf{R}^4}$ to the unit sphere. One has [12]

$$\Delta_{\mathcal{S}_3(0, R)} \equiv \Delta_{\mathcal{S}_3}/R^2 = \Delta_{\mathbf{R}^4} - \frac{\partial^2}{\partial R^2} - \frac{3}{R} \frac{\partial}{\partial R} .$$

Many theorems of vectorial analysis involving Beltrami operators find their counterpart in the space \mathcal{S}_3 . This is notably the case of the Green-Beltrami theorem which extends the well known Green's first identity [13] and is of an overwhelming importance to build the electrostatics in \mathcal{S}_3 . It reads [12]:

$$\int_{\mathcal{S}_3} d\Omega \nabla_{\mathcal{S}_3} f \cdot \nabla_{\mathcal{S}_3} g = - \int_{\mathcal{S}_3} d\Omega f \Delta_{\mathcal{S}_3} g , \quad (5)$$

where $f(\mathbf{z})$ and $g(\mathbf{z})$ are functions defined on the unit sphere \mathcal{S}_3 . The missing proof of theorem (5) (as well as the proofs of many other statements given in the sequel) is not so difficult and can be found in the recent textbook by Atkinson and Han [12].

C. Functions defined on $\mathcal{S}_3(O, R)$

The eigenfunctions of the Beltrami-Laplace operator $\Delta_{\mathcal{S}_3}$ are the 4D spherical harmonics $Y_{L,\alpha}(\mathbf{z})$ with eigenvalues $-L(L+2)$, $L = 0, 1, \dots$ being a positive integer; *i.e.* one has

$$\Delta_{\mathcal{S}_3} Y_{L,\alpha} = -L(L+2) Y_{L,\alpha} . \quad (6)$$

The degeneracy of the eigenvalue labelled by L is $(L+1)^2$ and the second "quantum" number α accounts for this degeneracy. Its precise algebraic structure depends of the representation of the spherical harmonics. Quite generally, in a space \mathbf{E}_3 of arbitrary dimension $D = 4$, the spherical harmonics $Y_{L,\alpha}(\mathbf{z})$ is a harmonic and homogeneous polynomial of D variables and degree L restricted to the unit sphere $\mathcal{S}_{(D-1)}$ (in this paper $D = 4$) [12]. This has the interesting consequence that $Y_{L,\alpha}(-\mathbf{z}) = (-1)^L Y_{L,\alpha}(\mathbf{z})$. Explicit expressions of the $Y_{L,\alpha}(\mathbf{z})$ in spherical coordinates will be found in Refs. [14–16] but are of little use in these lines. More important is the fact that the 4D spherical harmonics $Y_{L,\alpha}(\mathbf{z})$ constitute a complete basis set to expand functions $f(\mathbf{z})$ defined on the unit hypersphere \mathcal{S}_3 . Orthogonality and completeness relations take the following form:

$$\int_{\mathcal{S}_3} d\Omega Y_{L,\alpha}^*(\mathbf{z}) Y_{L',\alpha'}(\mathbf{z}) = \delta_{LL'} \delta_{\alpha\alpha'} , \quad (7a)$$

$$\sum_{L,\alpha} Y_{L,\alpha}^*(\mathbf{z}) Y_{L,\alpha}(\mathbf{z}') = \delta_{\mathcal{S}_3}(\mathbf{z}, \mathbf{z}') , \quad (7b)$$

where the delta function $\delta_{\mathcal{S}_3}(\mathbf{z}, \mathbf{z}') \equiv \delta(1 - \mathbf{z} \cdot \mathbf{z}')$ [12] has the usual convolution property

$$\int_{\mathcal{S}_3} d\Omega' f(\mathbf{z}') \delta_{\mathcal{S}_3}(\mathbf{z}, \mathbf{z}') = f(\mathbf{z}) . \quad (8)$$

The delta function on the sphere $\mathcal{S}_3(O, R)$ will be conveniently denoted by

$$\delta(M, M') = \delta_{\mathcal{S}_3}(\mathbf{z}, \mathbf{z}')/R^3. \quad (9)$$

Moreover, as in $D = 3$, the 4D harmonics satisfy a so-called addition theorem which reads:

$$\sum_{\alpha} Y_{L,\alpha}^*(\mathbf{z}) Y_{L,\alpha}(\mathbf{z}') = P_L(\mathbf{z} \cdot \mathbf{z}'), \quad (10a)$$

$$P_L(\cos(\psi)) = \frac{L+1}{2\pi^2} \frac{\sin((L+1)\psi)}{\sin \psi}, \quad (10b)$$

where the Tchebycheff polynomials of the second kind $P_L(\cos(\psi))$ play, in $D = 4$, the role devoted to the Legendre polynomials in $D = 3$.

D. Vectors and vector fields of $\mathcal{S}_3(O, R)$

By convention, a vector $\boldsymbol{\mu}$ of $\mathcal{S}_3(O, R)$ at point M should be an ordinary vector of the 3D Euclidian space $\mathcal{T}(M)$, tangent to the hypersphere at point M . Taking the scalar product of two vectors $\boldsymbol{\mu}_1$ and $\boldsymbol{\mu}_2$ located at two distinct points, M_1 and M_2 of $\mathcal{S}_3(O, R)$ needs some precaution. It first requires to perform a parallel transport of vector $\boldsymbol{\mu}_1$ from M_1 to M_2 along the geodesic M_1M_2 and then to take a 3D scalar product in space $\mathcal{T}(M_2)$. Thus [3, 11]

$$\langle \boldsymbol{\mu}_1, \boldsymbol{\mu}_2 \rangle = \tau_{12} \boldsymbol{\mu}_1 \cdot \boldsymbol{\mu}_2, \quad (11)$$

where, in the r.h.s. the dot denotes the usual scalar product of the Euclidian space $\mathcal{T}(M_2) \subset E_4$. Vector $\tau_{12} \boldsymbol{\mu}_1$ results from a transport of $\boldsymbol{\mu}_1$ from the space $\mathcal{T}(M_1)$ to the space $\mathcal{T}(M_2)$ along the geodesic M_1M_2 , keeping its angle with the tangent to the geodesic constant. Explicitely one has:

$$\tau_{12} \boldsymbol{\mu}_1 = \boldsymbol{\mu}_1 - \frac{\boldsymbol{\mu}_1 \cdot \mathbf{z}_2}{1 + \cos \psi_{12}} (\mathbf{z}_1 + \mathbf{z}_2) \quad (12)$$

One checks the following geometrical properties

$$\begin{aligned} \tau_{12} \boldsymbol{\mu}_1 \cdot \mathbf{z}_2 &= 0, \\ \tau_{12} \mathbf{t}_{12}(1) &= \mathbf{t}_{12}(2), \\ \tau_{12} \tau_{21} \boldsymbol{\mu}_1 &= \boldsymbol{\mu}_1. \end{aligned} \quad (13)$$

Finally, by taking into account Eq. (12), the scalar product (11) may be rewritten more explicitly as

$$\langle \boldsymbol{\mu}_1, \boldsymbol{\mu}_2 \rangle = \boldsymbol{\mu}_1 \cdot \boldsymbol{\mu}_1 - \frac{(\boldsymbol{\mu}_1 \cdot \mathbf{z}_2) \cdot (\boldsymbol{\mu}_2 \cdot \mathbf{z}_1)}{1 + \cos \psi_{12}} . \quad (14)$$

Besides the scalar fields of section (II C) one also needs to consider vector fields. An example will be a field of gradients. Let $f(\mathbf{z}_1, \mathbf{z}_2)$ be some scalar field of *two* variables defined on the unit sphere \mathcal{S}_3 . We suppose that the two-point function $f(\mathbf{z}_1, \mathbf{z}_2)$ is invariant under the rotations of the Euclidian space E_4 which leave the center O invariant (*i.e.* the rotations of the orthogonal group $\mathcal{O}(4)$). Therefore $f(\mathbf{z}_1, \mathbf{z}_2) \equiv \tilde{f}(\psi_{12})$ depends solely on the geodesic length ψ_{12} . Taking the gradients of $f(\mathbf{z}_1, \mathbf{z}_1)$ at points \mathbf{z}_1 or \mathbf{z}_2 defines two gradient fields, obviously given by:

$$\begin{aligned} \nabla_{\mathcal{S}_{3,1}} f(\mathbf{z}_1, \mathbf{z}_2) &= -\frac{\partial \tilde{f}(\psi_{12})}{\partial \psi_{12}} \mathbf{t}_{12}(\mathbf{z}_1) , \\ \nabla_{\mathcal{S}_{3,2}} f(\mathbf{z}_1, \mathbf{z}_2) &= +\frac{\partial \tilde{f}(\psi_{12})}{\partial \psi_{12}} \mathbf{t}_{12}(\mathbf{z}_2) . \end{aligned} \quad (15)$$

III. ELEMENTARY ELECTROSTATICS OF $\mathcal{S}_3(O, R)$

A. Poisson Equation

Given a charge distribution $\rho_{\mathcal{S}_3}(\mathbf{z})$ of \mathcal{S}_3 , the electric potential $V_{\mathcal{S}_3}(\mathbf{z})$ is defined to be the solution of Poisson's equation

$$\Delta_{\mathcal{S}_3} V_{\mathcal{S}_3} = -4\pi \rho_{\mathcal{S}_3} , \quad (16)$$

where the operator entering the r.h.s. of the equation is the Laplace-Beltrami operator of section (II B). We first note that making $f = 1$ and $g = V_{\mathcal{S}_3}$ in equation (5) implies that the integral of $\Delta_{\mathcal{S}_3} V_{\mathcal{S}_3}$ over the whole hypersphere is zero. It follows, as a consequence of Poisson's equation (16), that the total charge of the space must vanish. As already pointed out in the introduction, the potential of a single point charge is not defined in \mathcal{S}_3 . Elementary objects need be neutral. In this paper we consider electrostatics based on bi-charges [9].

B. Bi-charges and bi-dipoles

We first consider a bi-charge q at point M_0 of $\mathcal{S}_3(O, R)$, *i.e.* a dumbbell made of a point charge $+q$ at point M_0 and a point charge $-q$ at the antipodal point \overline{M}_0 , with $\mathbf{O}\overline{M}_0 =$

$-\mathbf{OM}_0$. It can be denoted as $(M_0, q) \cup (\overline{M}_0, -q)$. The potential $V_{M_0}(M)$ created by $(M_0, q) \cup (\overline{M}_0, -q)$ at a point M of $\mathcal{S}_3(O, R)$ satisfies to Poisson equation :

$$\Delta_{\mathcal{S}_3(0,R)} V_{M_0}(M) = -\frac{4\pi q}{R^3} (\delta_{\mathcal{S}_3}(\mathbf{z}, \mathbf{z}_0) - \delta_{\mathcal{S}_3}(\mathbf{z}, \overline{\mathbf{z}}_0)) , \quad (17)$$

with the obvious notations $\overline{\mathbf{z}}_0 = -\mathbf{z}_0 = -\mathbf{OM}_0/R$. Expanding both sides of (17) upon spherical harmonics yields [3] :

$$\begin{aligned} V_{M_0}(M) &= \frac{8\pi}{R} \sum'_{L,\alpha} \frac{1}{L(L+2)} Y_{L,\alpha}^*(\mathbf{z}_0) Y_{L,\alpha}(\mathbf{z}) \\ &= \frac{q}{R} \cot \psi_{M_0M} , \end{aligned} \quad (18)$$

where the prime affixed to the sum in (18) denotes the restriction that L is an odd, positive integer. Notice that the potential is singular for $\psi_{M_0M} = 0$ and $\psi_{M_0M} = \pi$. At a given $r = R\psi_{M_0M}$ and in the large R limit, one recovers the Euclidian behavior $V_{M_0}(M) \sim q/r$, and, at the antipodal point $V_{M_0}(M) \sim -q/r$ as expected.

The potential created at point M by a bi-dipole $\boldsymbol{\mu}_0$ located at point M_0 is now obtained by a standard limit process :

$$\begin{aligned} V_{M_0,\boldsymbol{\mu}_0}(M) &= \frac{\boldsymbol{\mu}_0}{R} \cdot \nabla_{\mathcal{S}_3,M_0} V_{M_0}(M) , \\ &= \frac{\mu}{R^2} \frac{1}{\sin^2(\psi_{M_0M})} \mathbf{s}_0 \cdot \mathbf{t}_{M_0M}(M_0) , \end{aligned} \quad (19)$$

where $\mathbf{s}_0 = \boldsymbol{\mu}_0/\mu$ is the direction of $\boldsymbol{\mu}_0$ and μ its modulus. It can be remarked that our bi-dipole can be seen as the dumbbell $(M_0, \boldsymbol{\mu}_0) \cup (\overline{M}_0, \boldsymbol{\mu}_0)$. The dipolar potential $V_{M_0,\boldsymbol{\mu}_0}(M)$ is of course a fundamental, non-isotropic solution of Laplace equation on the hypersphere. Note that in the limit $r = R\psi_{M_0M}$ fixed, $R \rightarrow \infty$, vector $\mathbf{t}_{M_0M}(M_0) \sim \widehat{\mathbf{r}} = \overrightarrow{M_0M}/M_0M$ and one recovers the Euclidian expression $V_{M_0,\boldsymbol{\mu}_0}(M) \sim \boldsymbol{\mu}_0 \cdot \widehat{\mathbf{r}}/r^2$ as expected.

The electric field created by the dipole is obtained by taking minus the gradient of $V_{M_0,\boldsymbol{\mu}_0}(M)$ at point M with the result :

$$\mathbf{E}_{M_0,\boldsymbol{\mu}_0}(M) = -\frac{1}{R} \cdot \nabla_{\mathcal{S}_3,M} V_{M_0}(M) = 4\pi \mathbf{G}_0(M, M_0) \cdot \boldsymbol{\mu}_0 , \quad (20)$$

where we have introduced the tensorial vectorial Green's function $\mathbf{G}_0(M, M_0)$ for which we can give two expressions :

$$\mathbf{G}_0(M, M_0) = \frac{1}{4\pi R^3} \frac{1}{\sin^3(\psi_{M_0M})} [3 \cos(\psi_{M_0M}) \mathbf{t}_{M_0M}(M) \mathbf{t}_{M_0M}(M_0) - \mathbf{U}_{\mathcal{S}_3}(\mathbf{z}) \cdot \mathbf{U}_{\mathcal{S}_3}(\mathbf{z}_0)] , \quad (21a)$$

$$= -\frac{2}{R^3} \sum_{L, \alpha} ' \frac{1}{L(L+2)} \nabla_{\mathcal{S}_3} Y_{L, \alpha}^*(\mathbf{z}) \nabla_{\mathcal{S}_3} Y_{L, \alpha}(\mathbf{z}_0) , \quad (21b)$$

as a short algebra will show.

We stress that $\mathbf{G}_0(M, M_0)$ is a 4D dyadic tensor of the type $\mathbf{A}(M)\mathbf{A}(M_0)$, $\mathbf{A}(M)$ and $\mathbf{A}(M_0)$ being two vectors tangent to the hypersphere at the points M and M_0 , respectively. It is easy to show that in the limit $\psi_{M_0M} \rightarrow 0$, $\mathbf{G}_0(M, M_0)$ tends to its Euclidian limit $\mathbf{G}_{0, \mathbf{R}^3}(M, M_0) = [-\mathbf{U}_{\mathcal{S}_3}(M) + 3\widehat{\mathbf{r}}\widehat{\mathbf{r}}]/(4\pi r^3)$, with as usual $\mathbf{r} = \overrightarrow{M_0M}$ and $\widehat{\mathbf{r}} = \mathbf{r}/r$. The distribution $\mathbf{G}_{0, \mathbf{R}^3}(M, M_0)$ has a singularity $-(1/3)\mathbf{U}\delta(\mathbf{r})$ [13, 20] and therefore $\mathbf{G}_0(M, M_0)$ is singular for $\psi_{M_0M} \rightarrow 0$, with the same singularity. It may be important to extract this singularity and to define a non-singular Green function $\mathbf{G}_0^\delta(M, M_0)$ by the relations

$$\mathbf{G}_0(M, M_0) = \mathbf{G}_0^\delta(M, M_0) + \frac{1}{3}\delta(M, M_0)\mathbf{U}_{\mathcal{S}_3}(\mathbf{z}) , \quad (22a)$$

$$\mathbf{G}_0^\delta(M, M_0) = \begin{cases} \mathbf{G}_0(M, M_0) & , \text{ for } R\psi_{M_0M} > \delta , \\ 0 & , \text{ for } R\psi_{M_0M} < \delta , \end{cases} \quad (22b)$$

where δ is an arbitrary small cut-off ultimately set to zero. It must be understood that any integral involving \mathbf{G}_0^δ must be calculated with $\delta \neq 0$ and then taking the limit $\delta \rightarrow 0$. Some useful mathematical properties of $\mathbf{G}_0(M, M_0)$ are derived in the appendix.

We end this section by *defining* the interaction of two bi-dipoles $(M_1, \boldsymbol{\mu}_1)$ and $(M_2, \boldsymbol{\mu}_2)$ as $W_{\boldsymbol{\mu}_1, \boldsymbol{\mu}_2} \equiv -\boldsymbol{\mu}_1 \cdot 4\pi \mathbf{G}_0(1, 2) \cdot \boldsymbol{\mu}_2$ which gives, more explicitly and with the help of Eq. (21a)

$$W_{\boldsymbol{\mu}_1, \boldsymbol{\mu}_2} = \frac{1}{R^3} \frac{1}{\sin^3 \psi_{12}} \left(\boldsymbol{\mu}_1 \cdot \boldsymbol{\mu}_2 - 3 \cos \psi_{12} (\mathbf{t}_{12}(1) \cdot \boldsymbol{\mu}_1) (\mathbf{t}_{12}(2) \cdot \boldsymbol{\mu}_2) \right) , \quad (23a)$$

$$= \frac{1}{R^3} \frac{1}{\sin^3 \psi_{12}} \left(\boldsymbol{\mu}_1 \cdot \boldsymbol{\mu}_2 + 3 \frac{\cos \psi_{12}}{\sin^2 \psi_{12}} (\boldsymbol{\mu}_1 \cdot \mathbf{z}_2) (\boldsymbol{\mu}_2 \cdot \mathbf{z}_1) \right) . \quad (23b)$$

Once again one recovers the well-known Euclidian limit $W_{\boldsymbol{\mu}_1, \boldsymbol{\mu}_2} \sim (1/r_{12}^3)[\boldsymbol{\mu}_1 \cdot \boldsymbol{\mu}_1 - 3(\boldsymbol{\mu}_1 \cdot \widehat{\mathbf{r}}_{12})(\boldsymbol{\mu}_2 \cdot \widehat{\mathbf{r}}_{12})]$ of the dipole-dipole interaction when $\psi_{12} \rightarrow 0$.

IV. POLAR FLUID IN $\mathcal{S}_3(O, R)$

A. Two models of polar hard spheres in $\mathcal{S}_3(O, R)$

We consider two versions of a fluid of N dipolar hard spheres in $\mathcal{S}_3(O, R)$.

1. Mono-dipoles

The first version is that already considered in Ref. [5]. The dipoles are formed from pseudo-charges and are confined on the surface of the hypersphere. They must be carefully distinguished from those of Sec. (III) which are formed from bi-charges and take the appearance of dumbbells of dipoles. In a given configuration of point-dipoles $\boldsymbol{\mu}_i$ located at the points $OM_i = R\mathbf{z}_i$ ($i = 1, \dots, N$) of $\mathcal{S}_3(O, R)$ the configurational energy reads

$$U = \frac{1}{2} \sum_{i \neq j}^N v_{\text{HS}}^{\text{mono}}(\psi_{ij}) + \frac{1}{2} \sum_{i \neq j}^N W_{\boldsymbol{\mu}_i, \boldsymbol{\mu}_j}^{\text{mono}}, \quad (24)$$

where $v_{\text{HS}}^{\text{mono}}(\psi_{ij})$ is the hard-core pair potential in $\mathcal{S}_3(O, R)$ defined by

$$v_{\text{HS}}^{\text{mono}}(\psi_{ij}) = \begin{cases} \infty & \text{if } \sigma/R > \psi_{ij}, \\ 0 & \text{otherwise,} \end{cases} \quad (25)$$

and $W_{\boldsymbol{\mu}_i, \boldsymbol{\mu}_j}^{\text{mono}}$ is the energy of a pair of mono-dipoles. Recall that

$$W_{\boldsymbol{\mu}_i, \boldsymbol{\mu}_j}^{\text{mono}} = \frac{1}{\pi R^3} \left[\frac{2}{\sin^2 \psi_{ij}} (\boldsymbol{\mu}_i \cdot \mathbf{z}_j)(\boldsymbol{\mu}_j \cdot \mathbf{z}_i) + f(\psi_{ij}) \left(\boldsymbol{\mu}_i \cdot \boldsymbol{\mu}_j + 3 \cot \psi_{ij} \frac{(\boldsymbol{\mu}_i \cdot \mathbf{z}_j)(\boldsymbol{\mu}_j \cdot \mathbf{z}_i)}{\sin \psi_{ij}} \right) \right] \quad (26)$$

with

$$f(\psi_{ij}) = \frac{1}{\sin \psi_{ij}} \left(\cot \psi_{ij} + \frac{\pi - \psi_{ij}}{\sin^2 \psi_{ij}} \right). \quad (27)$$

We want to stress that the electric potentials created by mono- and bi-dipoles are both fundamental solutions of Laplace-Beltrami equation in the space $\mathcal{S}_3(O, R)$. These solutions differ by their singularities at $\psi = 0$ (mono- and bi-dipoles) and $\psi = \pi$ (bi-dipoles). The resulting dipole-dipole interactions are quite different as apparent on Eqs. (23b) (bi-dipoles) and (26) (mono-dipoles). However it is noteworthy that both interactions indeed present the same Euclidian limit for $\psi_{ij} \rightarrow 0$.

A thermodynamic state of this model is characterized by a density $\rho^* = N\sigma^3/V$ where $V = 2\pi^2 R^3$ is the 3D surface of the hypersphere $\mathcal{S}_3(O, R)$ and a reduced inverse temperature μ^* with $\mu^{*2} = \mu^2/(k_B T \sigma^3)$ (k_B Boltzmann constant, T absolute temperature in Kelvin).

2. Bi-dipoles

The second version is that introduced in Sec. (III), *i.e.* a fluid of bi-dipoles confined on the surface of the hypersphere $\mathcal{S}_3(O, R)$. Clearly, as in the case of bi-charges (cf. [9]) both dipoles of the dumbbell must be embedded at the center of a hard sphere of diameter σ to avoid a collapse of the system. In a given configuration of N bi-dipoles $\boldsymbol{\mu}_i$ located at the points $OM_i = R\mathbf{z}_i$ ($i = 1, \dots, N$) of $\mathcal{S}_3(O, R)$ the configurational energy reads

$$U = \frac{1}{2} \sum_{i \neq j}^N v_{\text{HS}}^{\text{bi}}(\psi_{ij}) + \frac{1}{2} \sum_{i \neq j}^N W_{\boldsymbol{\mu}_i, \boldsymbol{\mu}_j}^{\text{bi}}, \quad (28)$$

where $v_{\text{HS}}^{\text{mono}}(\psi_{ij})$ is hard-core pair potential defined by

$$v_{\text{HS}}^{\text{bi}}(\psi_{ij}) = \begin{cases} \infty & \text{if } \sigma/R > \psi_{ij} \text{ or } \psi_{ij} > \pi - \sigma/R, \\ 0 & \text{otherwise,} \end{cases} \quad (29)$$

and the dipole-dipole interaction $W_{\boldsymbol{\mu}_i, \boldsymbol{\mu}_j}^{\text{bi}}$ is precisely that defined at Eq. (23b).

The interpretation of this seemingly strange model is the following. It is easily realized that the genuine domain occupied by the model is the northern hemisphere $\mathcal{S}_3(O, R)^+$ rather than the whole hypersphere. When a dipole $\boldsymbol{\mu}$ quits $\mathcal{S}_3(O, R)^+$ at some point M of the equator the same $\boldsymbol{\mu}$ reenters at the antipodal point \bar{M} . So bi-dipoles living on the whole sphere are equivalent to mono-dipoles living on a single hemisphere but with boundary conditions which ensure homogeneity and isotropy at equilibrium. Other boundary conditions ensuring homogeneity and isotropy could be invented but yield more complicated dipolar interactions.

A thermodynamic state of this model is now characterized by a density $\rho^* = N\sigma^3/V$ where $V = \pi^2 R^3$ is the 3D surface of the northern hemisphere $\mathcal{S}_3(O, R)^+$ and the reduced inverse temperature μ^* with $\mu^{*2} = \mu^2/(k_B T \sigma^3)$ as in Sec. (IV A 1).

B. Thermodynamics and structure

The thermal average of the energy per particle $u = \langle U \rangle / N$ as well as other thermodynamic quantities should be the same for both models in a given state (ρ^*, μ^{*2}) , at least in the

thermodynamic limit $N \rightarrow \infty$ with ρ^* fixed. We have checked this point by means of extensive MC simulations in the canonical ensemble and we postpone the discussion of these numerical experiments to Sec. (V).

The structure at equilibrium is also of prime importance [2, 17]. In the fluid phase of a molecular liquid of linear molecules the equilibrium pair correlation function can be expanded on a set of rotational invariants $\Phi^{lmn}(1, 2)$ [4, 18] as

$$g(1, 2) = g^{000}(r_{12})\Phi^{000}(1, 2) + h^{110}(r_{12})\Phi^{110}(1, 2) + h^{112}(r_{12})\Phi^{112}(1, 2) + \dots \quad (30)$$

with, in \mathcal{S}_3 [4],

$$\Phi^{000}(1, 2) = 1, \quad (31a)$$

$$\begin{aligned} \Phi^{110}(1, 2) &= \langle \mathbf{s}_1, \mathbf{s}_2 \rangle, \\ &= \mathbf{s}_1 \cdot \mathbf{s}_2 - \frac{1}{1 + \cos \psi_{12}} (\mathbf{s}_1 \cdot \mathbf{z}_2) (\mathbf{s}_2 \cdot \mathbf{z}_1), \end{aligned} \quad (31b)$$

$$\begin{aligned} \Phi^{112}(1, 2) &= 3 (\mathbf{s}_1 \cdot \mathbf{t}_{12}(1)) (\mathbf{s}_2 \cdot \mathbf{t}_{12}(2)) - \langle \mathbf{s}_1, \mathbf{s}_2 \rangle, \\ &= -\mathbf{s}_1 \cdot \mathbf{s}_2 - \frac{2 + \cos \psi_{12}}{\sin^2 \psi_{12}} (\mathbf{s}_1 \cdot \mathbf{z}_2) (\mathbf{s}_2 \cdot \mathbf{z}_1). \end{aligned} \quad (31c)$$

In the case of polar fluids only the projections $g^{000}(r_{12})$, $h^{110}(r_{12})$, and $h^{112}(r_{12})$ have a real physical significance. In $\mathcal{S}_3(O, R)$, these functions obviously depend on the sole $r_{12} = R\psi_{12}$ at equilibrium, *i.e.* the geodesic distance between the two particles (1, 2). For a fluid of mono-dipoles $0 < \psi_{12} < \pi$, however, for the fluid of bi-dipoles, only the range $0 < \psi_{12} < \pi/2$ is available, because of the special boundary conditions involved in the model. The projections $h^{110}(r_{12})$ and $h^{112}(r_{12})$ are given by [4]

$$\begin{aligned} h^{110}(r_{12}) &= 3 \int \frac{d\Omega_1}{4\pi} \int \frac{d\Omega_2}{4\pi} g(1, 2) \Phi^{110}(1, 2), \\ &= \frac{3V}{N(N-1)} \left\langle \sum_{i \neq j=1}^N \frac{\Phi^{110}(1, 2) \chi(\psi_{ij} - \psi_{12})}{4\pi R^3 \sin^2(\psi_{ij}) \delta\psi} \right\rangle. \end{aligned} \quad (32a)$$

$$\begin{aligned} h^{112}(r_{12}) &= \frac{3}{2} \int \frac{d\Omega_1}{4\pi} \int \frac{d\Omega_2}{4\pi} g(1, 2) \Phi^{112}(1, 2), \\ &= \frac{3V}{2N(N-1)} \left\langle \sum_{i \neq j=1}^N \frac{\Phi^{112}(1, 2) \chi(\psi_{ij} - \psi_{12})}{4\pi R^3 \sin^2(\psi_{ij}) \delta\psi} \right\rangle. \end{aligned} \quad (32b)$$

where Ω_i ($i = 1, 2$) denotes the spherical coordinates of vector \mathbf{s}_i in the local basis at point

N	βu^{mono}	βu^{bi}	ϵ^{mono}	ϵ^{bi}	#configs
128	$-2.77588 \pm 4.3\text{e-}4$	$-2.76979 \pm 4.9\text{e-}4$	36.41 ± 0.12	31.46 ± 0.10	1.3×10^9
250	$-2.76321 \pm 3.1\text{e-}4$	$-2.75771 \pm 2.8\text{e-}4$	35.09 ± 0.12	32.47 ± 0.11	2.5×10^9
432	$-2.75574 \pm 1.5\text{e-}4$	$-2.75106 \pm 1.2\text{e-}4$	34.09 ± 0.07	32.17 ± 0.09	12.1×10^9
686	$-2.75074 \pm 1.1\text{e-}4$	$-2.74675 \pm 1.0\text{e-}4$	33.17 ± 0.07	31.84 ± 0.09	22.0×10^9
1024	$-2.74724 \pm 1.2\text{e-}4$	$-2.74385 \pm 1.2\text{e-}4$	32.56 ± 0.11	31.77 ± 0.13	16.4×10^9
2000	$-2.74319 \pm 1.0\text{e-}4$	$-2.74078 \pm 1.3\text{e-}4$	31.76 ± 0.14	31.20 ± 0.18	16.0×10^9
4000	$-2.74029 \pm 1.1\text{e-}4$	$-2.73855 \pm 1.1\text{e-}4$	31.00 ± 0.21	1.09 ± 0.28	16.0×10^9
8000	$-2.73816 \pm 1.3\text{e-}4$	$-2.73712 \pm 1.1\text{e-}4$	31.04 ± 0.38	30.67 ± 0.42	16.0×10^9
∞	$-2.73626 \pm 2.0\text{e-}4$	$-2.73567 \pm 1.9\text{e-}4$	-	-	-

TABLE I: Number of particles, reduced energies per particle, dielectric constant, and number of configurations for mono- and bi-dipoles (\mathcal{S}_3) with electrostatic coupling $\mu^{*2} = 2$. Reported data are given with two standard deviations. TL data are extrapolated via a second order polynomial in N^{-1} from the four largest systems.

M_i , $\delta\psi$ is the bin size and χ is defined as

$$\chi(\psi - \psi_{12}) = \begin{cases} 1 & \text{if } \psi_{12} < \psi < \psi_{12} + \delta\psi \\ 0 & \text{otherwise.} \end{cases} \quad (33)$$

Clearly the pair potentials can be reexpressed in term of the invariants $\Phi^{110}(1, 2)$ and $\Phi^{112}(1, 2)$. One checks that

$$W_{\mu_1, \mu_2}^{\text{mono}} = \frac{\mu^2}{3\pi R^3} \left[f(\psi_{12}) (2\Phi^{112}(1, 2) - \Phi^{110}(1, 2)) - 2(1 + \cos \psi_{12}) (\Phi^{112}(1, 2) + \Phi^{110}(1, 2)) \right], \quad (34a)$$

$$W_{\mu_1, \mu_2}^{\text{bi}} = \frac{\mu^2}{3\pi R^3} \left[2(1 - \cos \psi_{12}) \Phi^{000}(1, 2) - (1 + 2 \cos \psi_{12}) \Phi^{112}(1, 2) \right]. \quad (34b)$$

C. Fulton's theory

The theory of the dielectric constant of a polar fluid in $\mathcal{S}_3(O, R)$ was obtained in Ref. [19] for the fluid of mono-dipoles. We extend this theory to the fluid of bi-dipoles in this Sec. As

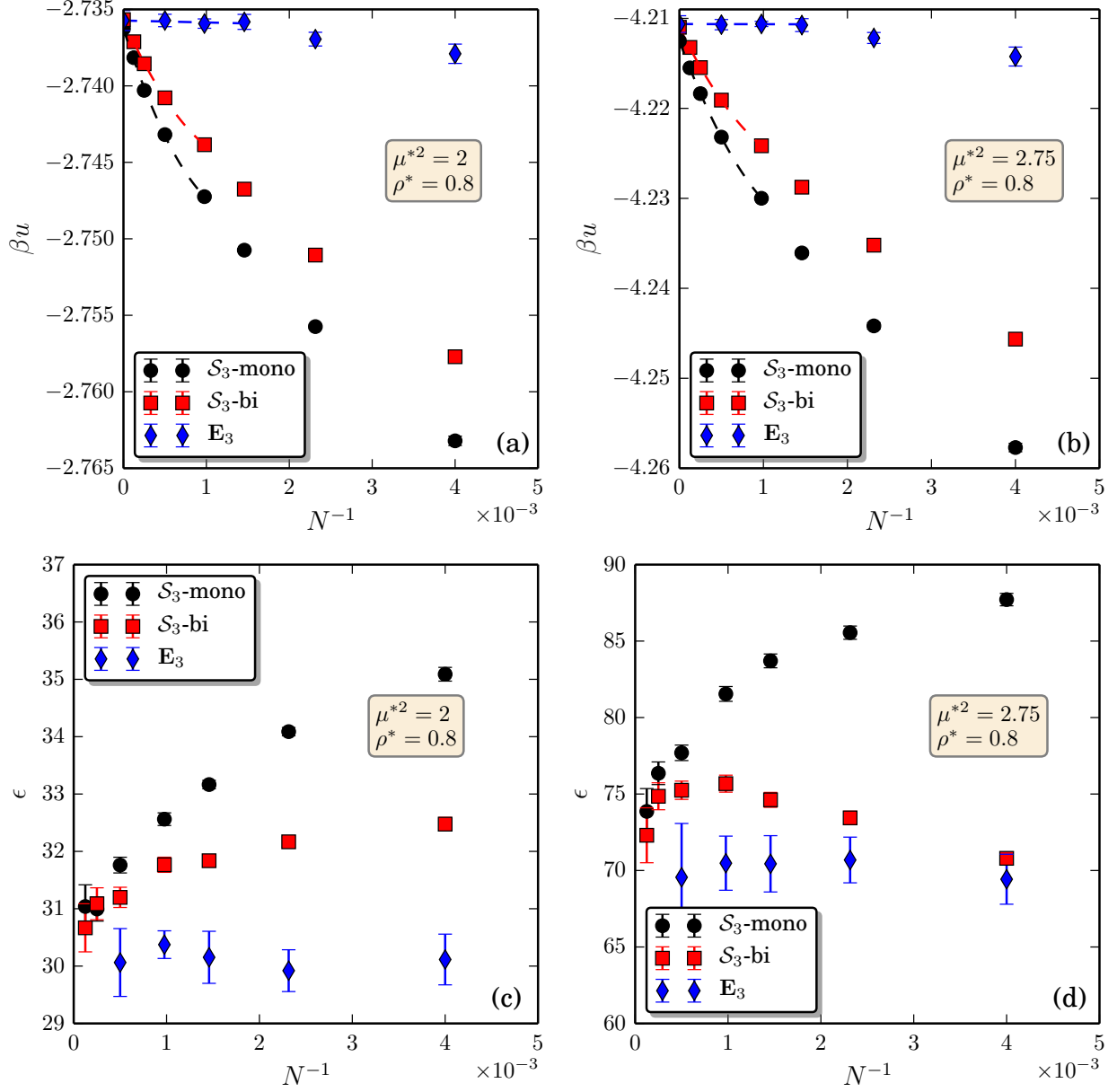


FIG. 1: Size convergence of both energies βu and dielectric constant ϵ for two considered thermodynamics states and for the three different potentials. Error bars correspond to two standard deviations. Dashed lines display a second/first order least square fit of the four/three largest systems ($\mathcal{S}_3/\mathbf{E}_3$).

in Ref. [19] we work in the framework of Fulton's theory which realizes a synthesis between linear response theory of dielectric media and electrodynamics [20]. We consider a fluid of N bi-dipoles in $\mathcal{S}_3^+(O, R)$ at thermal equilibrium in the presence of an external electrostatic field $\mathcal{E}(M) \in \mathcal{T}(M)$. This field is created for instance by a static distribution of bi-charges.

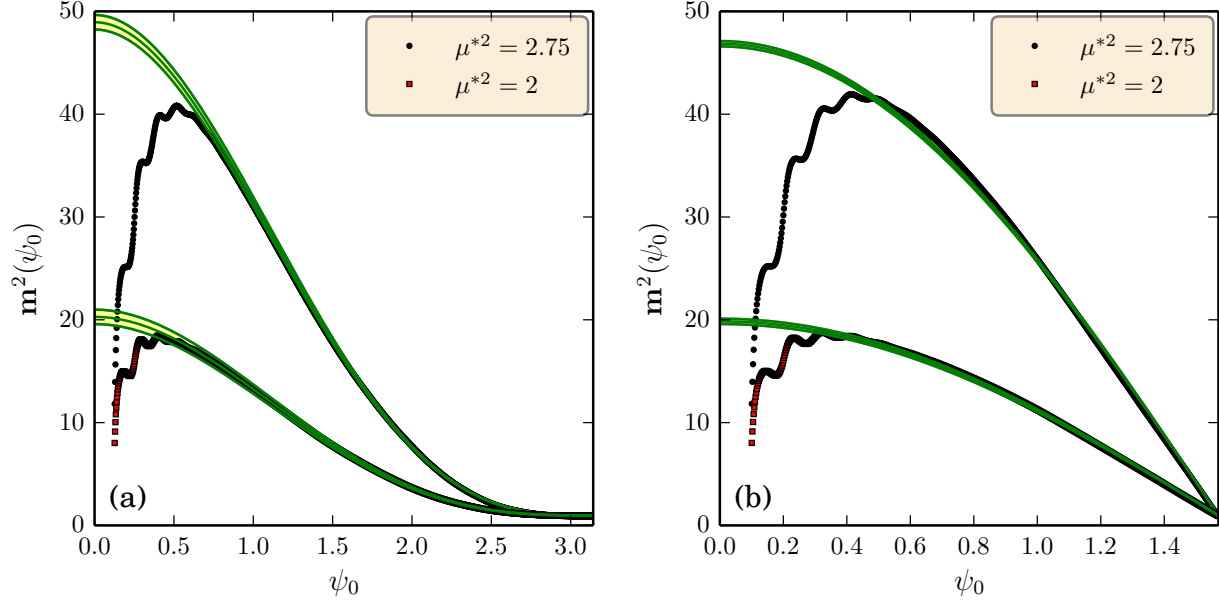


FIG. 2: Dipolar fluctuations m^2 as a function of angle ψ_0 for (a) mono-dipoles and (b) bi-dipoles. MC data are presented with markers while lines correspond to the analytic functions given by Eqs. (49) and (51). The lines are shown for ϵ values taken from Tables I and III with their upper and lower bounds.

N	βu	ϵ	#configs
128	$-2.74305 \pm 7.6e-4$	29.83 ± 0.29	3.8×10^8
250	$-2.73790 \pm 6.3e-4$	30.12 ± 0.44	7.5×10^8
432	$-2.73694 \pm 4.4e-4$	29.92 ± 0.36	1.3×10^9
686	$-2.73582 \pm 4.8e-4$	30.15 ± 0.44	2.1×10^9
1024	$-2.73593 \pm 3.0e-4$	30.37 ± 0.24	3.1×10^9
2000	$-2.73573 \pm 4.0e-4$	30.06 ± 0.59	2.0×10^9
∞	$-2.73573 \pm 6.5e-4$	-	-

TABLE II: Same as in table I for the Ewald potential (\mathbf{E}_3). TL data is extrapolated via a linear fit in N^{-1} from the three largest systems.

The medium then acquires a macroscopic polarization

$$\mathbf{P}(M) = \langle \hat{\mathbf{P}}(M) \rangle_{\epsilon}, \quad (35)$$

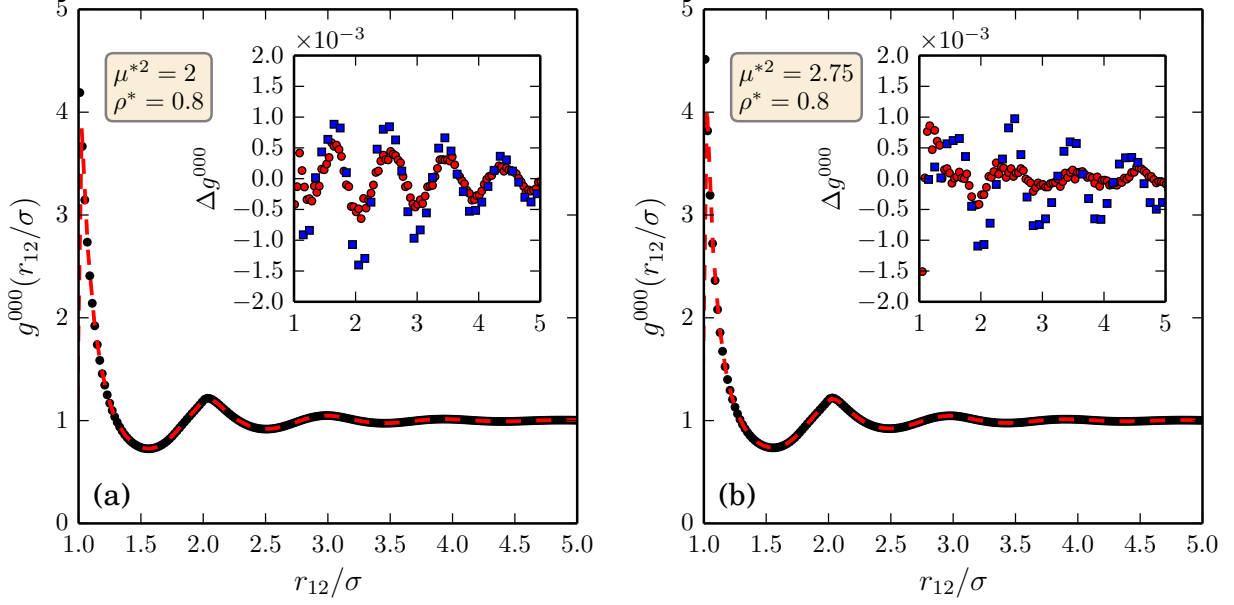


FIG. 3: Radial pair correlation functions g^{000} for 8000 bi-dipoles \mathcal{S}_3 -bi (black circles) and Ewald \mathbf{E}_3 (dashed red line) at $\rho^* = 0.8$ and for (a) $\mu^{*2} = 2$ and (b) $\mu^{*2} = 2.75$. *Insets:* show the differences (Δg^{000}) between \mathcal{S}_3 -bi and \mathcal{S}_3 -mono dipoles (red circles) and between \mathbf{E}_3 and \mathcal{S}_3 -mono dipoles (blue squares).

N	βu^{mono}	βu^{bi}	ϵ^{mono}	ϵ^{bi}	#configs
128	$-4.27856 \pm 6.7\text{e-}4$	$-4.26387 \pm 6.3\text{e-}4$	85.39 ± 0.33	62.27 ± 0.26	1.5×10^9
250	$-4.25770 \pm 4.7\text{e-}4$	$-4.24565 \pm 4.6\text{e-}4$	87.71 ± 0.41	70.80 ± 0.35	3.0×10^9
432	$-4.24418 \pm 3.5\text{e-}4$	$-4.23521 \pm 3.5\text{e-}4$	85.55 ± 0.43	73.44 ± 0.43	5.2×10^9
686	$-4.23607 \pm 2.8\text{e-}4$	$-4.22876 \pm 2.7\text{e-}4$	83.71 ± 0.45	74.62 ± 0.49	8.2×10^9
1024	$-4.23000 \pm 2.2\text{e-}4$	$-4.22416 \pm 2.2\text{e-}4$	81.54 ± 0.48	75.68 ± 0.56	12.3×10^9
2000	$-4.22320 \pm 1.6\text{e-}4$	$-4.21908 \pm 1.6\text{e-}4$	77.69 ± 0.50	75.25 ± 0.59	24.0×10^9
4000	$-4.21836 \pm 1.6\text{e-}4$	$-4.21547 \pm 1.6\text{e-}4$	76.36 ± 0.74	74.85 ± 0.88	24.0×10^9
8000	$-4.21550 \pm 1.9\text{e-}4$	$-4.21323 \pm 2.2\text{e-}4$	73.86 ± 1.49	72.30 ± 1.80	13.9×10^9
∞	$-4.21251 \pm 2.9\text{e-}4$	$-4.21098 \pm 3.2\text{e-}4$	-	-	-

TABLE III: Same as in Table I but for $\mu^{*2} = 2.75$.

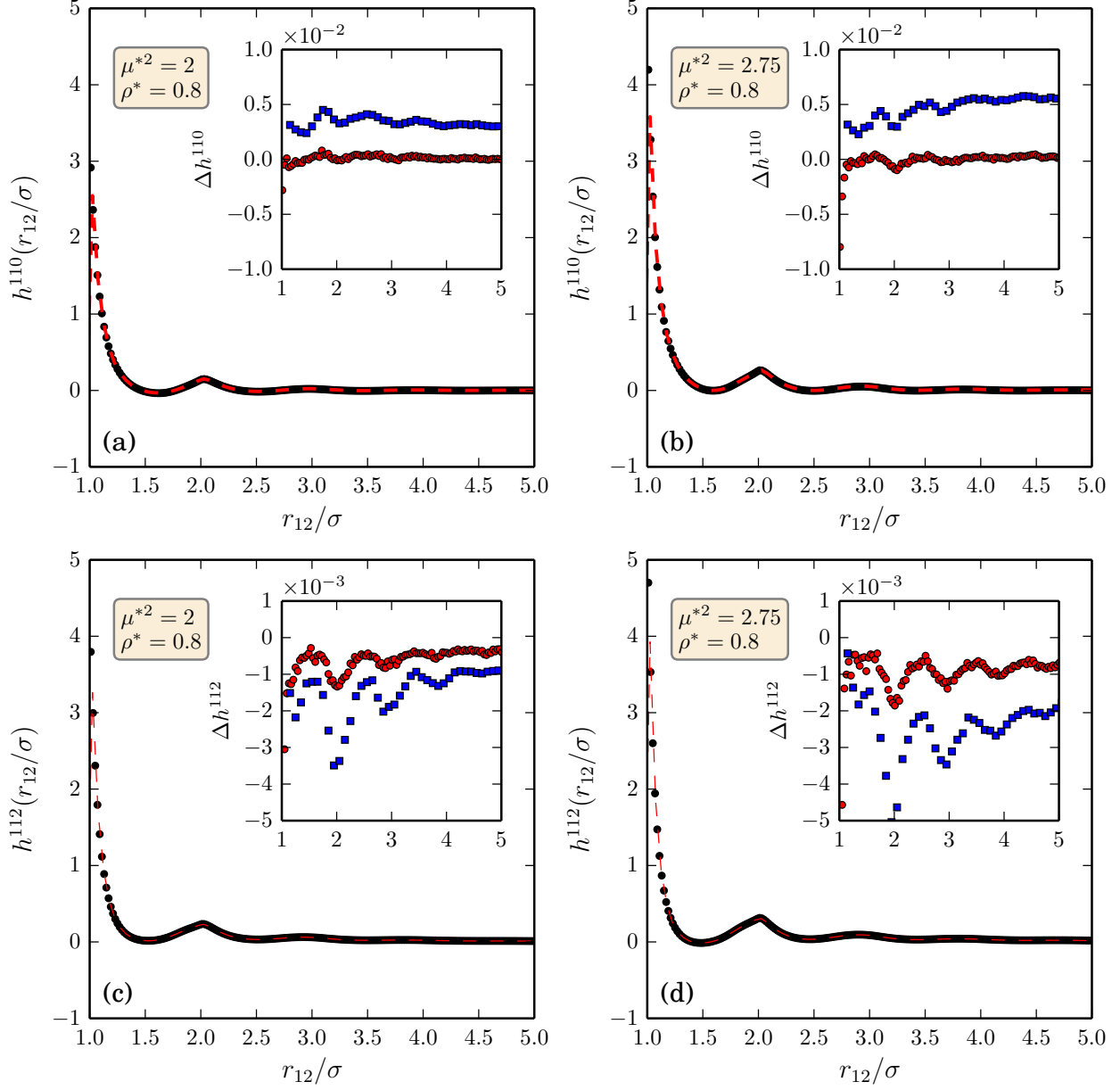


FIG. 4: Rotational invariants h^{110} and h^{112} for \mathcal{S}_3 -bi (black circles) and \mathbf{E}_3 (dashed red line) at the system size $N = 8000$ for the two systems. *Insets:* show the differences $\Delta h^{110/112}$ between \mathcal{S}_3 -bi and \mathcal{S}_3 -mono and (red circles) and between \mathbf{E}_3 and \mathcal{S}_3 -mono (blue squares).

where the brackets denote the equilibrium average of the dynamical variable $\widehat{\mathbf{P}}(M)$ in the presence of the external field \mathcal{E} . The microscopic polarization $\widehat{\mathbf{P}}(M)$ is defined in $\mathcal{S}_3(O, R)^+$ as

$$\widehat{\mathbf{P}}(M) = \sum_{j=1}^N \mathbf{U}_{\mathcal{S}_3}(\mathbf{z}) \cdot \boldsymbol{\mu}_j \delta(M, M_j). \quad (36)$$

N	βu	ϵ	#configs
128	$-4.22193 \pm 16.1\text{e-}4$	67.84 ± 1.40	3.8×10^8
250	$-4.21424 \pm 10.0\text{e-}4$	69.43 ± 1.63	7.5×10^8
432	$-4.21218 \pm 6.1\text{e-}4$	70.69 ± 1.49	1.3×10^9
686	$-4.21074 \pm 7.1\text{e-}4$	70.44 ± 1.84	2.1×10^9
1024	$-4.21062 \pm 2.9\text{e-}4$	70.48 ± 1.77	3.1×10^9
2000	$-4.21070 \pm 5.7\text{e-}4$	69.56 ± 3.51	2.0×10^9
∞	$-4.21063 \pm 9.2\text{e-}4$	-	-

TABLE IV: Same as Table II but for $\mu^{*2} = 2.75$.

The relation between the macroscopic polarization \mathbf{P} and the external field $\boldsymbol{\mathcal{E}}(M)$ can be established in the framework of linear-response theory (provided that $\boldsymbol{\mathcal{E}}(M)$ is small enough) with the result

$$4\pi\mathbf{P} = \boldsymbol{\chi} \circ \boldsymbol{\mathcal{E}} \left(\equiv \int_{\mathcal{S}_3(O,R)^+} d\tau(M') \boldsymbol{\chi}(M, M') \cdot \boldsymbol{\mathcal{E}}(M') \right). \quad (37)$$

The r.h.s. of Eq. (37) has been formulated in a compact, albeit convenient notation that will be adopted henceforth, where the symbol \circ means both a tensorial contraction (denoted by the dot " \cdot ") and a spacial convolution over the whole space (here $\mathcal{S}_3(O, R)^+$). From standard linear response theory the susceptibility $\boldsymbol{\chi}$ is given by

$$\boldsymbol{\chi}(M, M') = 4\pi\beta \langle \widehat{\mathbf{P}}(M) \widehat{\mathbf{P}}(M') \rangle, \quad (38)$$

where the thermal average $\langle \dots \rangle$ in the r.h.s. of (38) are evaluated in the absence of the external field and $\beta = 1/k_B T$. The dielectric properties of the fluid are characterized by the dielectric constant ϵ which however is described in a slightly different way than $\boldsymbol{\chi}$, according to the constitutive relation

$$4\pi\mathbf{P} = (\epsilon - \mathbf{I}) \circ \mathbf{E}, \quad (39)$$

where \mathbf{E} denotes the Maxwell field and $\mathbf{I}(M, M') \equiv \mathbf{U}_{\mathcal{S}_3(\mathbf{z})} \delta(M, M')$. In Eq. (39) the Maxwell field \mathbf{E} is the sum of the external field $\boldsymbol{\mathcal{E}}(M)$ and the induced field created by the macroscopic polarization \mathbf{P} . It is generally assumed that ϵ is a local function, *i.e.* $\epsilon = \epsilon \mathbf{I}$. More precisely, it is plausible -and we shall take it for granted- that $\epsilon(M, M')$ is a short

range function of the distance between the two points (M, M') , at least for a homogeneous liquid, and one then defines

$$\epsilon \mathbf{U}_{\mathcal{S}_3}(\mathbf{z}) = \int_{\mathcal{S}_3(O,R)^+} d\tau(M') \epsilon(M, M') \quad (40)$$

Obviously one has

$$\mathbf{E} = \boldsymbol{\mathcal{E}} + 4\pi \mathbf{G}_0 \circ \mathbf{P} , \quad (41)$$

where $\mathbf{G}_0(M, M')$ is the dipolar Green's function (21). In general $(\epsilon - \mathbf{I}) \neq \boldsymbol{\chi}$ since the Maxwell field $\mathbf{E}(M)$ and the external field $\boldsymbol{\mathcal{E}}(M)$ do not coincide. The relation between the two fields is easily obtained from (41) and usually recast as [19, 20]

$$\mathbf{E} = \boldsymbol{\mathcal{E}} + \mathbf{G} \circ \boldsymbol{\sigma} \circ \boldsymbol{\mathcal{E}} , \quad (42)$$

where $\boldsymbol{\sigma} \equiv \epsilon - \mathbf{I}$ and $\mathbf{G}(M, M')$ is the macroscopic dielectric Green's function defined by the identity

$$\mathbf{G} = \mathbf{G}_0 \circ (\mathbf{I} - \boldsymbol{\sigma} \circ \mathbf{G}_0)^{-1} . \quad (43)$$

To apprehend the physical significance of \mathbf{G} let us consider a point dipole $\boldsymbol{\mu}_0$ located at point M_0 of $\mathcal{S}_3(0, R)$. It creates an external field $\boldsymbol{\mathcal{E}}(M) = 4\pi \mathbf{G}_0(M, M_0) \cdot \boldsymbol{\mu}_0$. It follows then from Eq. (42) that the Maxwell field is given by

$$\mathbf{E}(M) = 4\pi (\mathbf{G}_0 + \mathbf{G} \circ \boldsymbol{\sigma} \circ \mathbf{G}_0)(M, M_0) \cdot \boldsymbol{\mu}_0 . \quad (44)$$

However $\mathbf{G} \circ \boldsymbol{\sigma} \circ \mathbf{G}_0 = \mathbf{G}_0 \circ [\mathbf{I} - \boldsymbol{\sigma} \circ \mathbf{G}_0]^{-1} \circ [\boldsymbol{\sigma} \circ \mathbf{G}_0 - \mathbf{I} + \mathbf{I}] = -\mathbf{G}_0 + \mathbf{G}$ from which it follows that $\mathbf{E}(M) = 4\pi \mathbf{G}(M, M_0) \cdot \boldsymbol{\mu}_0$ represents the electric field due to the dipole in the presence of the dielectric medium. Assuming the locality of the dielectric constant leads us to guess that for \mathcal{S}_3 , $\mathbf{G}(M, M_0) = \mathbf{G}_0(M, M_0)/\epsilon$ (in the absence of walls).

Combining Eqs. (37), (39), and (42) yields Fulton's relation

$$\boldsymbol{\chi} = \boldsymbol{\sigma} + \boldsymbol{\sigma} \circ \mathbf{G} \circ \boldsymbol{\sigma} . \quad (45)$$

To go further one has to compute seriously the macroscopic Green's function \mathbf{G} and check our guess. Our starting point is the following identity, proved in the appendix :

$$\mathbf{G}_0 \circ \mathbf{G}_0 = -\mathbf{G}_0 . \quad (46)$$

Therefore $-\mathbf{G}_0$ is a projector and has no inverse. Assuming the locality of $\boldsymbol{\sigma}$ one is then led to search the inverse $(\mathbf{I} - \boldsymbol{\sigma} \circ \mathbf{G}_0)^{-1}$ in the r.h.s. of (43) under the form $a\mathbf{I} + b\mathbf{G}_0$ where a

and b are numbers (or local operators). By identification one finds $a = 1$ and $b = \sigma/(1 + \sigma)$ yielding for \mathbf{G} the simple (and expected) expression

$$\mathbf{G} = \mathbf{G}_0/(1 + \sigma) \equiv \mathbf{G}_0/\epsilon. \quad (47)$$

This results allows to recast Fulton's relation (45) under its final form

$$(\epsilon - 1)\mathbf{I}(M_1, M_2) + \frac{(\epsilon - 1)^2}{\epsilon} \mathbf{G}_0(M_1, M_2) = \boldsymbol{\chi}(M_1, M_2). \quad (48)$$

We stress that the above equation has been obtained under the assumption of the locality of the dielectric tensor $\boldsymbol{\epsilon}(M, M')$. Therefore it should be valid only asymptotically, *i.e.* for points (M, M') at a mutual distance larger than the range ξ of $\boldsymbol{\epsilon}(M, M')$.

D. The dielectric constant and the Kirkwood's factor

Expressions for the dielectric constant, well suited for numerical simulations, can be obtained from Eq. (48) by integration. Slavishly following Refs. [19, 21] one integrates both sides of Eq. (48) and then takes the trace. The integration of M_2 is performed over a cone of axis \mathbf{z}_1 and aperture ψ_0 and then M_1 is integrated over the whole northern hemisphere $\mathcal{S}_3(O, R)^+$. The singularity of the dipolar Green's function $\mathbf{G}_0(M_1, M_2)$ for $\psi_{12} \sim 0$ must be carefully taken into account and this delicate point is detailed in the appendix (see Eq. (A.6)). One finds finally

$$\frac{\epsilon - 1}{\epsilon} + \frac{2(\epsilon - 1)^2}{3\epsilon} \cos \psi_0 = \mathbf{m}^2(\psi_0), \quad (49)$$

where the dipolar fluctuation $\mathbf{m}^2(\psi_0)$ reads as

$$\mathbf{m}^2(\psi_0) = \frac{4\pi\beta\mu^2}{3V} \left\langle \sum_i^N \sum_j^N \mathbf{s}_i \cdot \mathbf{s}_j \Theta(\psi_0 - \psi_{ij}) \right\rangle, \quad (50)$$

where $\Theta(x)$ is the Heaviside step-function ($\Theta(x) = 0$ for $x < 0$ and $\Theta(x) = 1$ for $x > 0$).

We have thus obtained a family of formula depending on parameter ψ_0 ; clearly they should be valid only if $R\psi_0$ is large when compared to the range of the dielectric constant. The numerical results of Sec. (V) show that this range is of the order of a few atomic diameters. It is also important to note that for $\psi_0 = \pi/2$ Eq. (49) involves the fluctuations of the total 4D dipole moment of the system. However, the resulting formula *i.e.* $(\epsilon - 1)/\epsilon = \mathbf{m}^2(\pi/2)$, albeit simple, is not adapted for numerical applications since, for large values of the dielectric

constant, a reasonable numerical error on ϵ requires a determination of $\mathbf{m}^2(\pi/2)$ with an impractical precision. The choice $\psi_0 = \pi/3$ yields the less simple formula $(\epsilon-1)(\epsilon+2)/(3\epsilon) = \mathbf{m}^2(\pi/3)$ which however allows, by contrast, a precise determination of ϵ . Indeed, let $\delta\epsilon$ be the error on ϵ , then, for high values of the dielectric constant the errors on $\mathbf{m}^2(\pi/3)$ and ϵ are roughly linearly proportional as $\delta\epsilon \sim 3 \delta\mathbf{m}^2(\pi/3)$

Note that formula (49) relating ϵ to the fluctuation $\mathbf{m}^2(\psi_0)$ are similar but not identical to that obtained for mono-dipoles [19] that we recall below for the sake of completeness :

$$\mathbf{m}^2(\psi_0) = \frac{\epsilon - 1}{\epsilon} + \frac{(\epsilon - 1)^2}{\epsilon} a(\psi_0) , \quad (51)$$

with

$$a(\psi) = \frac{2}{3\pi} (\sin \psi + (\pi - \psi) \cos \psi) . \quad (52)$$

The fluctuation $\mathbf{m}^2(\psi_0)$ is of course related to the Kirkwood factor $g^K(\psi_0)$. One has $\mathbf{m}^2(\psi_0) = 3yg^K(\psi_0)$, with $y = 4\pi\beta\rho\mu^2/9$ and

$$g^K(\psi_0) = 1 + \frac{\rho}{3} R^3 \int_0^{\psi_0} 4\pi \sin^2 \psi h^\Delta(\psi) d\psi , \quad (53)$$

where

$$h^\Delta(r = R\psi) = \frac{1}{3} (\cos \psi + 2) h^{110}(r) + \frac{2}{3} (\cos \psi - 1) h^{112}(r) . \quad (54)$$

It follows from (31) and (32) that

$$h^\Delta(r) = \frac{3V}{N(N-1)} \left\langle \sum_{i \neq j=1}^N \frac{(\mathbf{s}_i \cdot \mathbf{s}_j) \chi(\psi_{ij} - \psi)}{4\pi R^3 \sin^2(\psi_{ij}) \delta\psi} \right\rangle . \quad (55)$$

Note that in the thermodynamic limit (TL), *i.e.* fixed r and $R \rightarrow \infty$, one recovers the usual Euclidian expression of Kirkwood function [17]

$$h_\infty^\Delta(r) = \frac{3V}{N(N-1)} \left\langle \sum_{i \neq j=1}^N \frac{(\mathbf{s}_i \cdot \mathbf{s}_j) \chi(r_{ij} - r)}{4\pi r_{ij}^2 \delta r} \right\rangle , \quad (56)$$

where $\delta r = R\delta\psi$.

E. Asymptotic behavior of the pair correlation function.

Fulton's relation (48) has been used in Ref. [19] to obtain the asymptotic behavior of the projections $h^{110}(r)$ and $h^{112}(r)$ of the pair-correlation function $g(1,2)$ of a fluid of mono-dipoles. The extension of this analysis to a fluid of bi-dipoles is trivial and will not be

detailed here. Following step by step the derivations of Ref. [19] one easily obtains that, for large $r = R\psi$ and $\psi < \pi/2$, one should have asymptotically

$$h_{\text{asymp.}}^{110}(r) \sim -\frac{(\epsilon - 1)^2}{y\rho\epsilon} \frac{1}{4\pi R^3 \sin^3 \psi} \frac{2(1 - \cos \psi)}{3}, \quad (57a)$$

$$h_{\text{asymp.}}^{112}(r) \sim \frac{(\epsilon - 1)^2}{y\rho\epsilon} \frac{1}{4\pi R^3 \sin^3 \psi} \frac{1 + 2 \cos \psi}{3}. \quad (57b)$$

We stress that these asymptotic behaviors are valid, even for a finite radius R , as soon as $r \gg \xi$, where ξ denotes the range of the two point dielectric function $\epsilon(1, 2)$. Indeed they are easily obtained from Fulton's relation (48) which assumes the locality of $\epsilon(1, 2)$. This point is further discussed and confirmed by the MC simulations presented in Sec. (V). It must be stressed that, in the TL limit $R \rightarrow \infty$ and with $r \gg \xi$ fixed but large, one recovers the expected Euclidian behavior $h_{\text{asymp.}}^{112}(r) \sim (\epsilon - 1)^2 / (4\pi y\rho\epsilon) \times 1/r^3$ valid for an infinite system without boundaries at infinity [19, 22–24]. By contrast, in the same limit, one obtains that $h_{\text{asymp.}}^{110}(r) \sim (\epsilon - 1)^2 / (4\pi y\rho\epsilon) \times 1/r \times 1/R^2$ which tends to zero for the infinite system for which $R \rightarrow \infty$. This behavior is in agreement with the expected short range behavior of the projection $h^{110}(r)$ in the 3D infinite Euclidian space [22–24].

Let us now discuss the behavior of $h^\Delta(r)$. It follows from (57) that for $r \gg \xi$ one has

$$h_{\text{asymp.}}^\Delta(r) \sim -\frac{2}{3} \frac{(\epsilon - 1)^2}{y\rho\epsilon} \frac{1}{4\pi R^3 \sin \psi}. \quad (58)$$

As for $h^{110}(r)$, in the TL limit, $h_{\text{asymp.}}^\Delta(r) \rightarrow 0$ as R^{-2} at given r and $R \rightarrow \infty$.

Although the asymptotic tail of $h^\Delta(r)$ tends to zero uniformly in the limit $R \rightarrow \infty$, its integral over the volume of the cone of aperture ψ_0 in the r.h.s. of Eq. (49) gives a finite contribution to the Kirkwood function. Clearly, for large R , Eq. (53) can be written as

$$g^K(\psi_0) = g_\infty^K + \frac{\rho R^3}{3} \int_0^{\psi_0} h_{\text{asymp.}}^\Delta(r) 4\pi \sin^2(\psi) d\psi, \quad (59)$$

where g_∞^K is the Euclidian Kirkwood factor

$$g_\infty^K = \int_0^\infty 4\pi r^2 dr h_\infty^\Delta(r), \quad (60)$$

where $h_\infty^\Delta(r)$ is the infinite-volume limit of Kirkwood's pair correlations as defined in Eq. (56).

Now, inserting the asymptotic behavior (58) of $h^\Delta(r)$ in Eq. (59) one obtains

$$\frac{(\epsilon - 1)(2\epsilon + 1)}{\epsilon} = 9y g_\infty^K, \quad (61)$$

which is the well-known Kirkwood formula for the dielectric constant of an infinite Euclidian polar fluid without boundaries at infinity [17]. The above mechanism to get rid of the electrostatic tail of $h_{\text{asympt.}}^{\Delta}(r)$ in order to obtain the more intrinsic expression (61) of the dielectric constant, also works for mono-dipoles in $\mathcal{S}_3(0, R)$ or cubico-periodical geometries for which a similar explicit calculation can be performed (but will not be reported here due to lack of space). It is likely to be a general mechanism for any arbitrary, Euclidian or not, geometries.

V. MONTE CARLO SIMULATIONS

We performed standard Metropolis MC simulations of a DHS fluid with single particle displacements (translation and rotation), where each new configuration is generated by a trial displacement of *one* dipole. Two different systems were studied, both with the same reduced particle density $\rho^* = 0.8$, but with different reduced dipolar couplings, $\mu^{*2} = 2$ and $\mu^{*2} = 2.75$. These systems have previously been studied in the literature [26, 27] and serve as a good benchmark for any new potential. Both systems are known to be in the dielectric fluid phase [2, 28] (in contrast to a ferroelectric phase). The system sizes were systematically varied and the energies and dielectric constants extrapolated to their thermodynamic limits. Simulations were either performed on the hypersphere \mathcal{S}_3 or in the Euclidian space \mathbf{E}_3 with cubic periodic boundary conditions. Interaction potentials for the the mono- and bi-dipoles on \mathcal{S}_3 are given by Eq. (26) and (23b) while in \mathbf{E}_3 the dipolar Ewald summation techniques [2, 28] were applied. The parameters for the dipolar Ewald potential were adapted from an automatic scheme for charged particles [29] using a real-space cut-off equal to half the box-length. Systematic tests were performed to ensure that the resulting energies and dielectric constants were not influenced by the chosen precision of the dipolar Ewald method (within error bars). The data presented for the Ewald method were obtained with tinfoil boundary conditions, split parameters α in the range $[1.150994\sigma^{-1}, 0.480594\sigma^{-1}]$, and with a number of wave-functions in the range [871, 1059] for systems between $N = 128$ and 2000 dipoles.

Below we give results from extensive simulations of DHS in \mathcal{S}_3 and \mathbf{E}_3 geometries at different system sizes. MC data for the energy and the dielectric constant are given in Tabs. I-IV for the two thermodynamic states ($\rho^* = 0.8, \mu^{*2} = 2$) and ($\rho^* = 0.8, \mu^{*2} = 2.75$) for the three potentials and various number of particles N as well as the extrapolation to

$N \rightarrow \infty$.

The energies and the dielectric constants all converge, as expected, to the same values in the thermodynamic limit for all three potentials (see Fig. (1) and Table I-IV). The energies can be well fitted with $\beta u = \beta u_\infty + \mathcal{O}(1/N)$ for the largest system sizes (for our purpose we used a second order polynomial in $1/N$). We were incapable to perform a similar analysis for the dielectric constant due to larger error bars but it seems reasonable to assume that the thermodynamic limit is close to the value obtained for $N = 8000$ particles. We found $\{\beta u_\infty = -2.736 \pm 0.001, \epsilon \simeq 30 \pm 2\}$ and $\{\beta u_\infty = -4.212 \pm 0.002, \epsilon \simeq 70 \pm 5\}$ for the two considered states. These values are considerably more precise than previous studies of the same systems [26, 27] and serve as an update of these thermodynamic values. From Fig. (1) one finds that the \mathbf{E}_3 and the Ewald summation techniques tends to give faster size convergence (to the TL), which seems to have converged both in energy and dielectric constant already at a system sizes around $N \sim 700$.

Note that the dielectric constant in Figure (2) and Tables I-IV are calculated from Eqs. (51) and (49) at the specific angles $\psi_0 = \pi/2$ for \mathcal{S}_3 -mono and $\psi_0 = \pi/3$ for \mathcal{S}_3 -bi. However, when the fluctuations of the dipole moment are integrated over volumes corresponding to other values of the angle ψ_0 the same dielectric constant is obtained as soon as ψ_0 is large enough as can be seen in Fig. (2). Only at small ψ_0 , i.e. for $R\psi_0 < \xi$ (ξ range of dielectric constant) do the fluctuations differ from the predictions of macroscopic (local) electrostatics given by Eqs. (51) and (49), due to short-ranged molecular structuring and orientally ordering.

Figs. (3) and (4) display the isotropic correlation functions $g^{000}(r)$ and the projections $h^{110}(r)$ and $h^{112}(r)$ and show a very good agreement with very small structural and orientally differences (less than 10^{-2} units) between the two different geometries (\mathcal{S}_3 and \mathbf{E}_3) at short separations for all the three different potentials (\mathcal{S}_3 -mono, \mathcal{S}_3 -bi, and \mathbf{E}_3) considered here. The slightly larger discrepancy between the Ewald potential compared to the two hypersphere potentials is most likely due the smaller size in the former ($N = 2000$ compared to $N = 8000$).

As discussed in Sec. (IV E) small differences should exist in the asymptotic regime which are dictated by the geometry. Indeed, one finds the expected behavior (57) as apparent in Figs. (5) and (6). The two projections $h^{110}(r)$ and $h^{112}(r)$ tend towards their asymptotic predictions for distances $r_{12} > \zeta$ (i.e. $h_{MC}^{mnl}/h_{\text{asympt.}}^{mnl} \simeq 1$ as $r_{12} > \xi$), where $\xi \sim 7\sigma$ for the

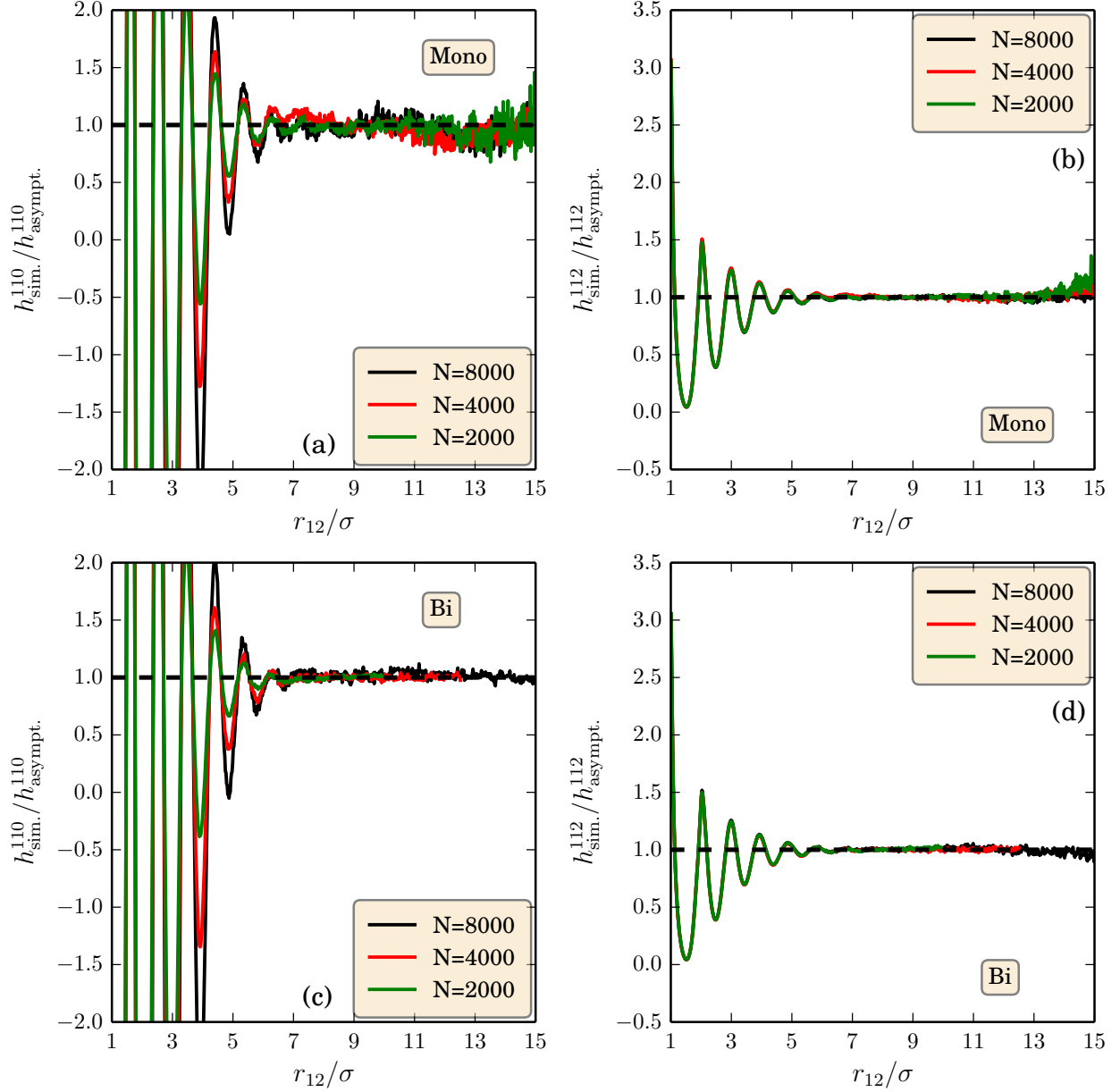


FIG. 5: Asymptotic behavior of the rotational invariants. $h^{110}(r)/h_{\text{asympt.}}^{110}(r)$ and $h^{112}(r)/h_{\text{asympt.}}^{112}(r)$ for (a,b) \mathcal{S}_3 -mono and (c,d) \mathcal{S}_3 -bi for $\mu^{*2} = 2$. Lines as in Fig. 4 but for the Eqs. (57) in this paper and Eqs. (4.32) from [19].

two considered states. Notice that the values of $h_{\text{MC}}^{110}/h_{\text{asympt.}}^{110}$ at short separations diverges, as $h_{\text{asympt.}}^{110} \rightarrow 0$ when $R \rightarrow \infty$.

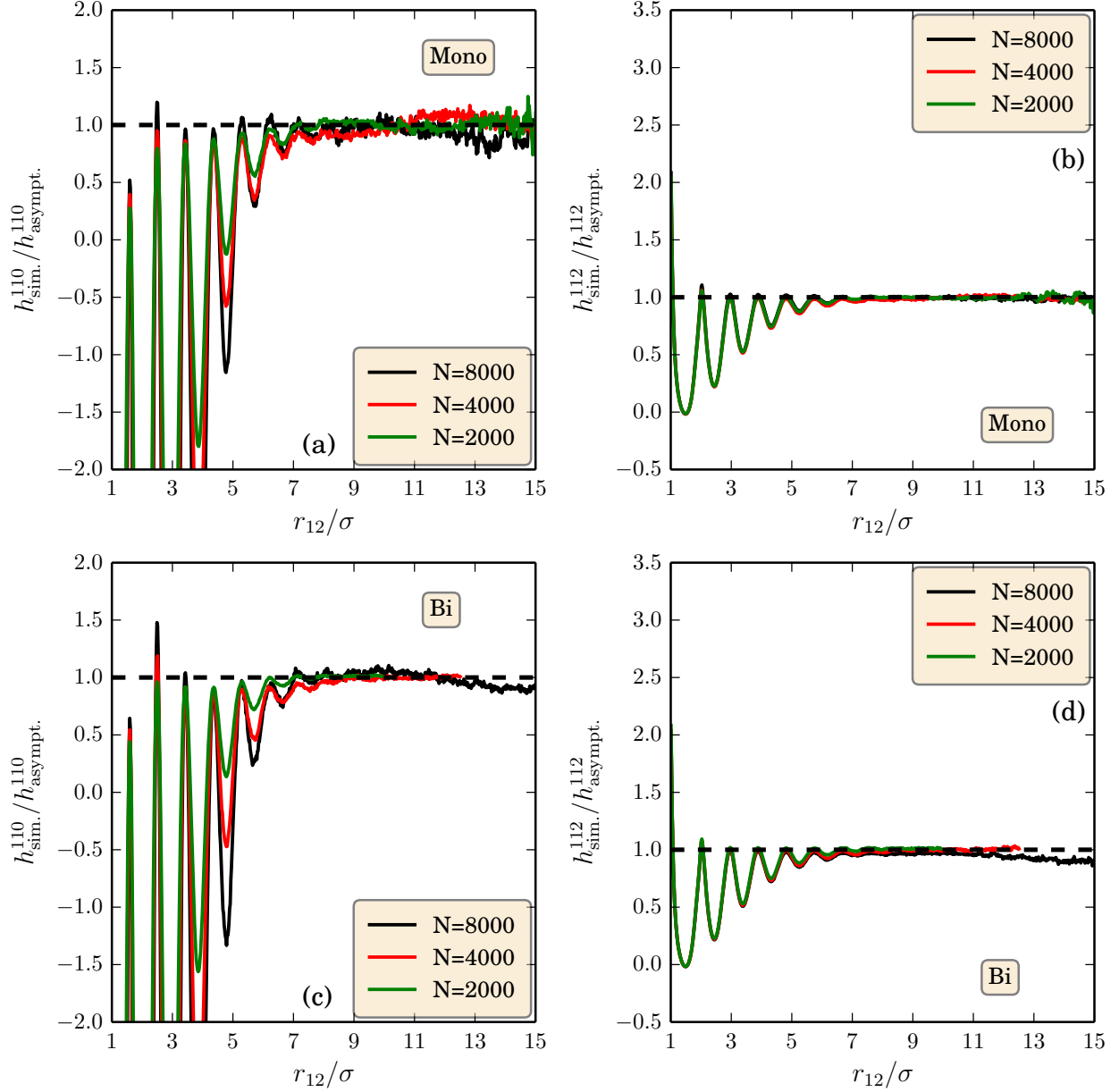


FIG. 6: Same as Fig. (5) with $\mu^{*2} = 2.75$

VI. CONCLUSION

We have introduced a new method of simulation for dipolar liquids on the hypersphere $S_3(0, R)$. We have noted that, in this geometry, the electrostatics can be built in two different ways. Starting from pseudo-charges we obtain mono-dipoles : the potential of such a dipole is a solution of Laplace-Beltrami equation with a single singularity at the origin. Bi-dipoles are obtained from bi-charges and are more elaborated since their electric potential, although

also a solution of Laplace-Beltrami equation, exhibits two singularities, one at the origin and the other at the antipodal point. A dipolar fluid can thus be represented as an assembly of mono-dipoles living in $\mathcal{S}_3(0, R)$ (the volume of the system is then $2\pi^2 R^3$) or a collection of bi-dipoles living in the northern hemisphere $\mathcal{S}_3(0, R)^+$ (the volume of the system is now $\pi^2 R^3$). Of course these elaborated boundary conditions apply to ensure, in the absence of external fields or walls, the homogeneity of the fluid : when a dipole leaves the hemisphere $\mathcal{S}_3(0, R)^+$ at some point M of the equator it reenters $\mathcal{S}_3(0, R)^+$ at the antipodal point \bar{M} , bearing the same dipole. Of course mixture of bi-charges and bi-dipoles could be considered to simulate symmetric models of electrolytes.

Since the Green's function of Laplace-Beltrami is explicitly known both for mono- and bi-dipoles the theory of the dielectric constant of the homogeneous fluid can be done in great details in both cases, including the derivation of the tail of the equilibrium pair correlation function induced by the curvature. Moreover we were able to extract the contributions of these tail to the Kirkwood's factor in the TL and thus to recover the well known Kirkwood's expression of the dielectric constant for a fluid filling the ordinary infinite Euclidian space.

We have reported MC data for simulations of two states of the fluid of dipolar hard spheres and performed systematic investigation of a novel potential on the hypersphere consisting of bi-dipoles. The great efficiency of the simulations on the hypersphere allows a drastic reduction of the numerical uncertainties on the data. As far as the energy is concerned, the $1/N$ dependence on the MC data has been obtained for the largest systems yielding precise estimates of its thermodynamic limit, with a relative precision of $\sim 10^{-4}$. For both considered states, the TL on the energy coincide for mono and bi-dipoles in \mathcal{S}_3 within the error bars; they are also in good agreement with the data obtained in cubico-periodic geometries together with the use of Ewald potentials. It seems that the TL limit is reached faster in the latter case, however the relative precision on the Ewald potential (for a discussion see Ref. [28]) is of the same order of magnitude than the precision that we obtained for the TL limit of the energy in our simulation in \mathcal{S}_3 , which should temper the adepts of the former method. The numerical uncertainties on the dielectric constant preclude a similar study of its thermodynamic limit. As a remark : even at small system sizes (for instance $N = 128$) one does not find errors greater than 2% (compared to the TL) in energy and 20% in the dielectric constant.

We have also checked the prediction of Sec. (IV E) on the behavior of the tails of the

angular correlation functions. The agreement between the theoretical predictions and the results of simulations is quite excellent and gives insight on the (short) range of the dielectric tensor $\epsilon(1, 2)$. Theoretical efforts are still needed to obtain an explicit expression of $\epsilon(1, 2)$ which should allow its complete calculation in a MC simulation.

It is difficult to assess the relative merits of mono or bi-dipoles. The convergence towards the TL seems however slightly, but marginally faster for bi-dipoles. Clearly both methods do not surpass the standard Ewald summation techniques in size convergence. However on the hypersphere the dipole-dipole interactions can be computed, directly or with the help of tabulations, with an arbitrary precision by contrast with the Ewald potential which allways involves systematic numerical errors [28]. In cases where the precision on the pair potential is crucial the hypersphere technology should be preferred.

Acknowledgments

We thank D. Levesque and J.-J. Weis for providing us a MC code of dipolar hard spheres with Ewald potentials that we used for a part of the numerical experiments on the state ($\rho^* = 0.8, \mu^{*2} = 2$). J.-M. Caillol acknowledges D. Levesque for his enlightened advises, interest and encouragements.

Appendix: Some properties dipolar Green's functions in \mathcal{S}_3

First we shall prove that, with M_1 and M_2 being two points of the Northern hemisphere of the unit hypersphere \mathcal{S}_3^+ , we have

$$[\mathbf{G}_0 \circ \mathbf{G}_0](1, 2) = \int_{\mathcal{S}_3^+} d\Omega(3) \mathbf{G}_0(1, 3) \cdot \mathbf{G}_0(3, 2) = -\mathbf{G}_0(1, 2) . \quad (\text{A.1})$$

We rewrite eq (21b) as

$$\mathbf{G}_0(1, 2) = \sum_{L, \alpha} ' \mathbf{G}_0^{L, \alpha}(1, 2) , \quad (\text{A.2})$$

with

$$\mathbf{G}_0^{L, \alpha}(1, 2) = -\frac{2}{L(L+2)} \nabla_{\mathcal{S}_3} Y_{L, \alpha}^*(\mathbf{z}_1) \nabla_{\mathcal{S}_3} Y_{L, \alpha}(\mathbf{z}_2) . \quad (\text{A.3})$$

Since for an odd L , $Y_{L,\alpha}(-\mathbf{z}) = -Y_{L,\alpha}(\mathbf{z})$ one has

$$\int_{\mathcal{S}_3^+} d\Omega(\mathbf{z}) \mathbf{G}_0^{L,\alpha}(1,3) \cdot \mathbf{G}_0^{L',\alpha'}(3,2) = \frac{4}{L(L+2)L'(L'+2)} \nabla_{\mathcal{S}_3} Y_{L,\alpha}^*(\mathbf{z}_1) \nabla_{\mathcal{S}_3} Y_{L',\alpha'}(\mathbf{z}_2) \times \\ \times \frac{1}{2} \int_{\mathcal{S}_3} d\Omega(\mathbf{z}) \nabla_{\mathcal{S}_3} Y_{L,\alpha}(\mathbf{z}_3) \cdot \nabla_{\mathcal{S}_3} Y_{L',\alpha'}^*(\mathbf{z}_3). \quad (\text{A.4})$$

The integral in Eq. (A.4) is computed by applying the Green-Beltrami identity (5) and the properties (6) and (7a) of the spherical harmonics giving us

$$\int_{\mathcal{S}_3} d\Omega(\mathbf{z}) \nabla_{\mathcal{S}_3} Y_{L,\alpha}(\mathbf{z}) \cdot \nabla_{\mathcal{S}_3} Y_{L',\alpha'}^*(\mathbf{z}) = L(L+2) \delta_{L,L'} \delta_{\alpha,\alpha'}. \quad (\text{A.5})$$

Inserting Eq.(A.5) in Eq.(A.4) readily yields the announced result (A.1).

Our second result concern the integration of $\mathbf{G}_0(1,2)$ on a cone of axis \mathbf{z}_1 and aperture $0 \leq \psi_0 \leq \pi/2$. We shall prove that

$$\int_{0 \leq \psi_{12} \leq \psi_0} d\Omega(\mathbf{z}_2) \mathbf{G}_0(1,2) = \left(-1 + \frac{2}{3} \cos \psi_0\right) \mathbf{U}_{\mathcal{S}_3}(\mathbf{z}_1). \quad (\text{A.6})$$

To prove Eq. (A.6) one needs to take some precaution because of the singularity of $\mathbf{G}_0(1,2)$ at $\psi_{12} = \cos^{-1}(\mathbf{z}_1 \cdot \mathbf{z}_2) \rightarrow 0$. We make use of the decomposition (22a) to rewrite

$$\int_{0 \leq \psi_{12} \leq \psi_0} d\Omega(\mathbf{z}_2) \mathbf{G}_0(1,2) = -\frac{1}{3} \mathbf{U}_{\mathcal{S}_3}(\mathbf{z}_1) + \lim_{\delta \rightarrow 0} \int_{\delta \leq \psi_{12} \leq \psi_0} d\Omega(\mathbf{z}_2) \mathbf{G}_0(1,2). \quad (\text{A.7})$$

The integral in the r.h.s. of Eq. (A.7) is computed by using spherical coordinates to reexpress the formula (21b) of the Green function and performing explicetly the integrals. A short computation gives us

$$\int_{\delta \leq \psi_{12} \leq \psi_0} d\Omega(\mathbf{z}_2) \mathbf{G}_0(1,2) = \frac{2}{3} (\cos \psi_0 - \cos \delta) \mathbf{U}_{\mathcal{S}_3}(\mathbf{z}_1), \quad (\text{A.8})$$

with a well-behaved limit $\delta \rightarrow 0$. Combining Eqs. (A.7) and (A.8) indeed yields the desired result (A.6).

In this appendix we implicitly assumed that $R = 1$. The reassessment of Eqs. (A.1) and (A.6) in the case $R \neq 1$ is however trivial since the dipolar Green's function $\mathbf{G}_0(1,2)$ scales as R^{-3} with the radius of the sphere. Clearly Eqs. (A.1) and (A.6) remain valid for $R \neq 1$ with the replacement $d\Omega(\mathbf{z}) \rightarrow d\tau(M)$ where $d\tau(M) = R^3 d\Omega(\mathbf{z})$ is the infinitesimal volume element of the sphere $\mathcal{S}_3(O, R)$ of radius R .

-
- [1] S. W. de Leeuw, J. W. Perram, and E. R. Smith, Proc. R. Soc. London Ser. A **373**, 27 (1980); **373**, 47 (1980).
- [2] J.-J. Weis and D. Levesque, in *Advanced Computer Simulation*, edited by C. Holm and K. Kremer, Vol. **185**, 163 (Springer Verlag, 2005).
- [3] J.-M. Caillol and D. Levesque, J. Chem. Phys. **94**, 597 (1991).
- [4] J.-M. Caillol, J. Chem. Phys. **96**, 1455 (1992).
- [5] J.-M. Caillol and D. Levesque, J. Chem. Phys. **96**, 1477 (1992).
- [6] M. Trulsson, J. Chem. Phys., **133**, 174105 (2010).
- [7] L. Landau and E. Lifchitz, *The Classical Theory of Fields* (Pergaman, New York, 1962).
- [8] J.-M. Caillol and D. Gilles, J. Phys. A: Math. Theor. **43**, 105501 (18pp) (2010).
- [9] J.-M. Caillol, J. Chem. Phys., **99**, 8953 (1993).
- [10] J.-M. Caillol, D. Levesque, and J.-J. Weis, J. Chem. Phys. **116**, 10794-10800 (2002).
- [11] J.-M. Caillol, D. Levesque, and J.-J. Weis, Mol. Phys. **44**, 733 (1981).
- [12] K. Atkinson and W. Han, *Spherical Harmonics and Approximations on the Unit Sphere : an Introduction* (Lecture Notes in Mathematics, 2044, Springer, Berlin Heidelberg, 2012).
- [13] J. D. Jackson, *Classical Electrodynamics* (John Wiley & Sons, New York, 1962).
- [14] N. K. Vilenkin, Am. Math. Soc. Transl., **22** (1968).
- [15] J. Avery, *Hyperspherical Harmonics, Applications to Quantum Theory* (Kluwer, Dordrecht, The Netherlands, 1989)
- [16] Higuchi Atsuchi, J. Math. Phys. **28**, 7 (1987).
- [17] J.-P. Hansen and I. R. McDonald, *Theory of Simple Liquids* (3rd Ed., Academic Press, London, 2006).
- [18] L. Blum and A. J. Torruella, J. Chem. Phys. **56**, 303 (1972).
- [19] J.-M. Caillol, J. Chem. Phys. **96**, 7039 (1992).
- [20] R. L. Fulton, J. Chem. Phys. **68**, 3089 (1978); **68**, 3095 (1978); **78**, 6865 (1983).
- [21] H. J. C. Berendsen, Molecular Dynamics and Monte Carlo Calculations on Water, Cecam Report (1972), p.21.
- [22] G. Nienhuis and J. M. Deutch, J. Chem. Phys. **55**, 4213 (1971); **56**, 5511 (1972).
- [23] J. S. Høye and G. Stell, J. Chem. Phys. **61**, 562 (1974); **64**, 1952 (1976)

- [24] G. Stell, G. N. Patey, and J. S. Høye, *Adv. Chem. Phys.* **38**, 183 (1981).
- [25] M. Neumann and O. Steinhauser, *Chem. Phys. Lett.* **95**, 417 (1982).
- [26] D. J. Adams, *Mol. Phys.* **40**, 1261 (1980).
- [27] G. N. Patey, D. Levesque, and J.-J. Weis, *Mol. Phys.* **45**, 733 (1982).
- [28] C. Holm and J.-J. Weis, *Curr. Opinion Coll. and Int. Sci.* **10**, 133 (2005).
- [29] P. Linse, *Adv. in Polymer Science*, Vol. **85**, (Springer, Berlin, 2005).